# Energy, Mass, Time, Space

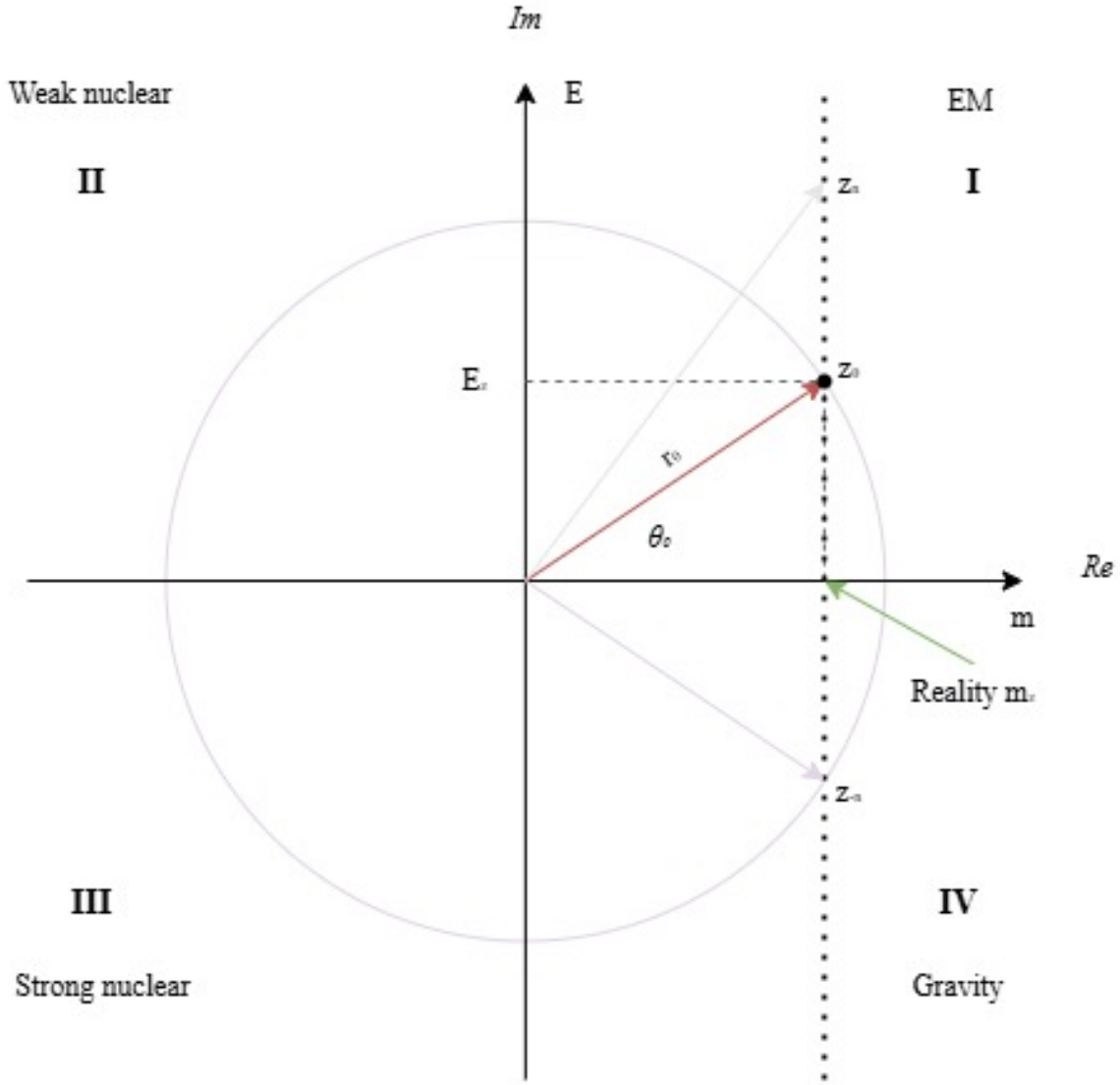




Compiled on February 24, 2026

*To life.*

# Contents

# License

This work is licensed under the Creative Commons Attribution-ShareAlike 4.0 International (CC BY-SA 4.0).
SPDX-License-Identifier: CC-BY-SA-4.0
The full license text from the repository is reproduced below.

```
Creative Commons Attribution-ShareAlike 4.0 International (CC BY-SA 4.0)

SPDX-License-Identifier: CC-BY-SA-4.0

Copyright (c) 2025 Giancarlo Trevisan

This work is licensed under the Creative Commons Attribution-ShareAlike 4.0
International License.

You are free to:
- Share - copy and redistribute the material in any medium or format
- Adapt - remix, transform, and build upon the material for any purpose, even commercially

Under the following terms:
- Attribution - You must give appropriate credit, provide a link to the license, and
        indicate if changes were made.
- ShareAlike - If you remix, transform, or build upon the material, you must distribute
        your contributions under the same license as the original.

No additional restrictions - You may not apply legal terms or technological measures that
legally restrict others from doing anything the license permits.

Full legal code: https://creativecommons.org/licenses/by-sa/4.0/legalcode

Human-readable summary: https://creativecommons.org/licenses/by-sa/4.0/

a. Adapted Material means material subject to Copyright and Similar Rights that is derived
from or based upon the Licensed Material and in which the Licensed Material is translated,
altered, arranged, transformed, or otherwise modified in a manner requiring permission
under the Copyright and Similar Rights held by the Licensor. For purposes of this Public
License, where the Licensed Material is a musical work, performance, or sound recording,
Adapted Material is always produced where the Licensed Material is synched in timed
relation with a moving image.

b. Adapter's License means the license You apply to Your Copyright and Similar Rights in
Your contributions to Adapted Material in accordance with the terms and conditions of
this Public License.

c. BY-SA Compatible License means a license listed at
creativecommons.org/compatiblelicenses, approved by Creative Commons as essentially the
equivalent of this Public License.

d. Copyright and Similar Rights means copyright and/or similar rights closely related to
```

# Preface

In scientific discovery, pure mathematics often serves as the bedrock of our understanding of the universe. This essay is my attempt to develop, in real time with AI, an idea that has echoed in my mind for years. It is a perspective, not a declaration, and simply asks, *what if?*

> Don't think it doesn't make sense; ask yourself what sense it could have.

First, a mathematical framework is defined that ties Energy, Mass, Time and Space (EMTS), then speculates how the framework could fit with our knowledge.

Giancarlo Trevisan

*Visualize then Realize!*

# Part I

# Foundations

# Chapter 1

# The Complex Plane

The connection between the complex plane and reality becomes especially significant when we consider the origins and applications of imaginary numbers. Historically, the introduction of imaginary numbers emerged from attempts to solve cubic equations, as first systematically explored by Gerolamo Cardano in the 16th century. Cardano discovered that even when all solutions to a cubic equation were real, the algebraic process sometimes required passing through intermediate steps involving the square roots of negative numbers—quantities that had no clear interpretation at the time.

This mathematical curiosity turned out to be much more than a formal trick. The development of complex numbers enabled mathematicians and physicists to describe phenomena that could not be captured by real numbers alone. A profound example is the discovery of electromagnetic waves. In the 19th century, James Clerk Maxwell formulated his famous equations, which describe how electric and magnetic fields propagate and interact. The solutions to Maxwell's equations are most naturally expressed using complex exponentials, where the imaginary unit i encodes oscillatory behavior—essential for describing wave phenomena such as light and radio waves (see Maxwell's equations[6]).

Thus, imaginary numbers are not merely abstract constructs; they are indispensable tools for modeling and understanding the physical world. Their use reveals that reality possesses layers and symmetries that extend beyond direct sensory perception, hinting at a deeper mathematical structure underlying the universe. The complex plane, therefore, is not just a mathematical convenience but a window into the hidden fabric of nature.

The complex plane, a mathematical construct that allows us to visualize complex numbers as points in a two-dimensional space. In this plane, the horizontal axis represents the real numbers, while the vertical axis represents the imaginary numbers. For our purposes, we will map mass onto the real axis and energy onto the imaginary axis. Why this choice? Well, mass seems more real than energy from my point of view (feel free to swap). With this picture in mind, let's pick a point $z_0$ on the complex plane and dive into its possible implications.

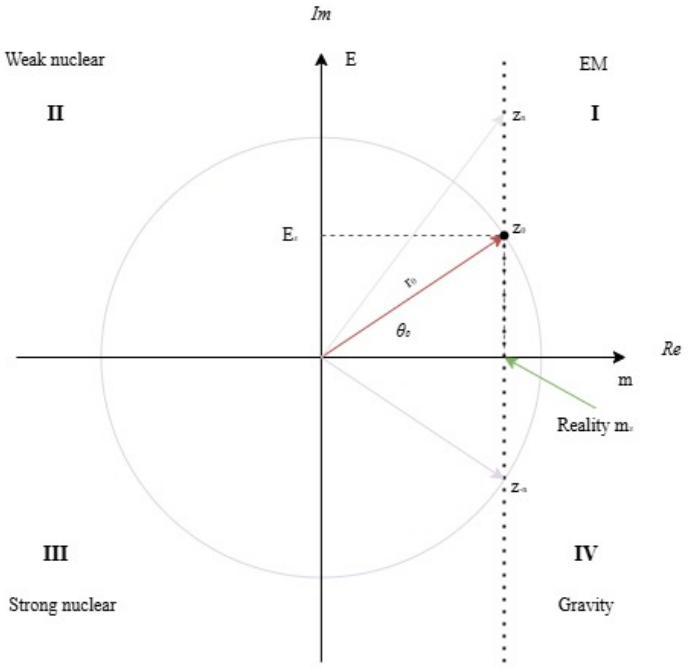


Figure 1.1: Complex plane illustration. $m_z$ is what we perceive at time $\theta_0$ and space $r_0$.

# Chapter 2

# The EMTS Framework: Core Definitions

Having introduced the complex plane and its historical significance, we now establish the foundational elements of the Energy-Mass-Time-Space (EMTS) framework. This chapter consolidates the core mathematical definitions and physical interpretations that underpin the entire theory.

## 2.1 The complex plane mapping

The EMTS framework posits that physical states can be represented as points in the complex plane:

$$z = m + iE,$$

where:

- $m$ is the mass component (mapped to the real axis)
- $E$ is the energy component (mapped to the imaginary axis)
- $i = \sqrt{-1}$ is the imaginary unit

This choice reflects the intuition that mass is "more tangible" than energy in everyday experience, though the mapping could be reversed without loss of generality. What matters is the *relationship* between the components, not which axis they occupy.

## 2.2 Polar representation

Every complex point $z$ can be expressed in polar form:

$$z = re^{i\theta} = r(\cos\theta + i\sin\theta),$$

where:

- $r = |z| = \sqrt{m^2 + E^2}$ is the **modulus** (unified magnitude)
- $\theta = \arg(z) = \arctan(E/m)$ is the **argument** (unified phase)

### 2.2.1 Physical interpretation of $r$ and $\theta$

The modulus $r$ represents the total mass-energy content:

$$r = \sqrt{(mc^2)^2 + E^2} \quad \text{or in natural units} \quad r = \sqrt{m^2 + E^2}.$$

The argument $\theta$ encodes the **partition** between mass and energy:

$$m = r\cos\theta, \tag{2.1}$$
$$E = r\sin\theta. \tag{2.2}$$

Crucially, we identify $\theta$ with time evolution:

$$\theta(t) = \omega t,$$

where $\omega$ is the angular frequency related to energy by $E = \hbar\omega$ (Planck's quantum hypothesis).

### 2.2.2 The projection principle

**Central postulate:** Physical reality corresponds to the *projection* of the complex state onto the real axis:

$$\text{Observable reality} = \Re(z) = m = r\cos\theta.$$

This projection is **many-to-one**: infinitely many complex states

$$\{z_n = m + iE_n\}_n$$

all project to the same observable value $m$. The imaginary component $E$ represents hidden degrees of freedom that influence dynamics but are not directly observed.

## 2.3 Fundamental relationships

### 2.3.1 Time as phase

The identification $\theta = \omega t$ unifies time evolution with rotation in the complex plane. A state evolves as:

$$z(t) = re^{i\omega t}.$$

The observable projection oscillates:

$$m(t) = r\cos(\omega t),$$

explaining wave-like behavior from the geometry of rotation.

### 2.3.2 Energy-frequency connection

From quantum mechanics:

$$E = \hbar\omega \quad \Rightarrow \quad \omega = \frac{E}{\hbar}.$$

Thus the rotation rate in the complex plane is proportional to energy, linking dynamics to the imaginary component.

### 2.3.3 Measurement and collapse

In standard quantum mechanics, measurement "collapses" the wavefunction. In the EMTS framework:

1. Before measurement: Full state is $z = m + iE$ with complex dynamics
2. Measurement: Projects to $\Re(z) = m$
3. After measurement: The imaginary component $E$ remains but is decohered from the observable $m$

Multiple branches with different $E$ values persist along the imaginary axis (see Chapter 7 for the multiverse interpretation).

## 2.4 Force quadrants

The complex plane is divided into four quadrants based on the sign of $m$ and $E$. We hypothesize that fundamental forces correspond to phase windows:

| Quadrant | Force | Phase Range | Symbol |
|---|---|---|---|
| I | Electromagnetic | $0 < \theta < \frac{\pi}{2}$ | $Q_{\text{I}}$ |
| II | Weak | $\frac{\pi}{2} < \theta < \pi$ | $Q_{\text{II}}$ |
| III | Strong | $\pi < \theta < \frac{3\pi}{2}$ | $Q_{\text{III}}$ |
| IV | Gravitational | $\frac{3\pi}{2} < \theta < 2\pi$ | $Q_{\text{IV}}$ |

Each force is characterized by a phase window $W_f(\theta)$ and coupling function $g_f(\theta, r)$. The observed interaction strength depends on where the state $z(t)$ resides in the phase cycle (see Chapter 5 for details).

## 2.5 Notation conventions

Throughout this work, we use the following notation:

- $z = m + iE = re^{i\theta}$ — Complex state (canonical form: $z = m + iE = re^{i\theta}$)
- $\theta = \omega t$ — Phase-time relation (shorthand: $\theta = \omega t$)
- $r = |z|$ — Modulus (total mass-energy)
- $\Re(z) = r\cos\theta = r\cos\theta$ — Real projection (observable)
- $\Psi(z, t)$ or $\Psi(r, \theta)$ — Wavefunction on complex state space
- $Q_{\text{I}}, Q_{\text{II}}, Q_{\text{III}}, Q_{\text{IV}}$ — Force quadrants (EM, Weak, Strong, Gravitational)

## 2.6 Relationship to standard physics

The EMTS framework is not a replacement for quantum mechanics or relativity, but a *geometric reinterpretation* that:

- Recovers the Schrödinger equation in appropriate limits
- Naturally incorporates special relativity through $r = \sqrt{m^2 + E^2}$
- Provides a unified language for discussing particles, forces, and spacetime
- Suggests extensions (e.g., multiverse structure, dark matter) that emerge from the geometry

Standard formulations are recovered by:

1. Restricting to the real axis (classical limit)
2. Quantizing the phase $\theta$ (quantum mechanics)
3. Coupling the modulus $r$ to spacetime curvature (general relativity)

## 2.7 Summary: The EMTS postulates

We summarize the core framework:

1. **Complex representation**: Physical states are complex numbers $z = m + iE$
2. **Polar dynamics**: States evolve as $z(t) = re^{i\omega t}$ with $\omega = E/\hbar$
3. **Projection principle**: Observable reality is $\Re(z)$; imaginary components are hidden
4. **Phase-force mapping**: Forces correspond to phase windows in $[0, 2\pi)$
5. **Quantization**: Periodicity in $\theta$ leads to discrete spectra
6. **Dimensionality from precision**: Effective dimensionality increases with measurement precision

The remaining chapters develop these postulates in detail, exploring their implications for quantum mechanics (Part I), the Standard Model (Part II), specific phenomena (Part III), and future directions (Part IV).

# Chapter 3

# Polar Representation and Its Implications

Building on the core framework (Chapter 2), we explore deeper implications of the polar representation $z = m + iE = re^{i\theta}$. This chapter examines how the modulus $r$ and argument $\theta$ relate to physical measurements and quantum phenomena.

## 3.1 Extended physical interpretation

The modulus $r = \sqrt{m^2 + E^2}$ and argument $\theta = \arctan(E/m)$ were defined and given their primary physical interpretation in Section 2.2 of Chapter 2. In SI units ($c \neq 1$) these generalise to $r = \sqrt{(mc^2)^2 + E^2}$ and $\theta = \arctan(E/mc^2)$. This chapter builds directly on that foundation, extending the physical interpretation rather than re-deriving it.

**Space and Time.** The key relation $\theta = \omega t$ with $E = \hbar\omega$ means probabilities or densities linked to projections oscillate with $\omega$. The projection $m_z = \Re(z) = r\cos\theta$ can repeat with period $2\pi$ even as the underlying phase history differs.

**Projection as Measurement.** With the unit vector $|\psi\rangle = \cos\theta\,|m\rangle + i\sin\theta\,|E\rangle$, a mass measurement uses $P_m$ and yields $\mathbb{P}(m) = \cos^2\theta$, mirroring $m_z = r\cos\theta$. Standard treatments of such two-level mappings can be found in Griffiths[4].

# Chapter 4

# Hermitian Operators on a Hilbert Space

The EMTS framework posits that physical states are complex numbers $z = m + iE$, rotating in the complex plane as time advances. This geometric picture demands a rigorous operator-theoretic scaffolding: *which* quantities are observable, *how* are they extracted from a complex state, and *why* do measurements always return real values? The answer lies in the theory of Hermitian operators acting on a Hilbert space. This chapter builds that theory from first principles, continuously anchoring each definition to the EMTS picture.

## 4.1 The EMTS Hilbert Space

The appropriate arena for EMTS quantum states is the two-dimensional complex Hilbert space

$$\mathcal{H} = \mathbb{C}^2,$$

equipped with the standard inner product

$$\langle \phi | \psi \rangle = \phi_1^* \psi_1 + \phi_2^* \psi_2, \qquad \phi, \psi \in \mathcal{H}.$$

We choose an **EMTS basis** that reflects the physical partition of mass and energy:

$$|m\rangle = \begin{pmatrix} 1 \\ 0 \end{pmatrix}, \qquad |E\rangle = \begin{pmatrix} 0 \\ 1 \end{pmatrix}.$$

These basis vectors are orthonormal, $\langle m|m\rangle = \langle E|E\rangle = 1$ and $\langle m|E\rangle = 0$, and they span $\mathcal{H}$ completely: any state can be written as a superposition

$$|\psi\rangle = \alpha\,|m\rangle + \beta\,|E\rangle, \qquad \alpha, \beta \in \mathbb{C}.$$

### 4.1.1 Normalized EMTS states

Physical states carry unit norm. Demanding $\langle \psi | \psi \rangle = 1$ constrains $|\alpha|^2 + |\beta|^2 = 1$, which is solved by

$$|\psi\rangle = \cos\theta\,|m\rangle + i \sin\theta\,|E\rangle, \qquad \theta \in [0, 2\pi).$$

The single real parameter $\theta$ encodes the entire state:

- $\theta = 0$: pure mass state $|m\rangle$—fully real, directly observable.

- $\theta = \pi/2$: pure energy state $i|E\rangle$—fully imaginary, hidden from direct observation.
- $0 < \theta < \pi/2$: superposition carrying both mass and energy character.

This parametrisation directly mirrors the EMTS complex representation $z = m + iE = re^{i\theta}$, where $\cos\theta$ and $\sin\theta$ govern the mass-energy partition at any instant.

## 4.2 Linear Operators on $\mathcal{H}$

A **linear operator** $A : \mathcal{H} \to \mathcal{H}$ is a $2 \times 2$ complex matrix acting on kets:

$$A|\psi\rangle = \begin{pmatrix} A_{11} & A_{12} \\ A_{21} & A_{22} \end{pmatrix} \begin{pmatrix} \alpha \\ \beta \end{pmatrix}.$$

The **adjoint** (Hermitian conjugate) $A^\dagger$ is defined by the inner-product relation

$$\langle \phi | A\psi \rangle = \langle A^\dagger \phi | \psi \rangle \quad \forall\, \phi, \psi \in \mathcal{H},$$

which for $2 \times 2$ matrices reduces to $A^\dagger = (A^*)^T$: transpose, then complex-conjugate each entry.

### 4.2.1 Key operator classes

| Class | Condition | Role in EMTS |
|---|---|---|
| Hermitian | $A^\dagger = A$ | Observables (real eigenvalues) |
| Unitary | $U^\dagger U = \mathbf{1}$ | Time evolution (norm-preserving) |
| Projection | $P^2 = P,\ P^\dagger = P$ | Measurement outcomes |

All three classes appear naturally in EMTS: observables are Hermitian, time evolution is unitary, and each measurement outcome is selected by a projection operator.

## 4.3 Hermitian Operators and Observables

An operator $A$ is **Hermitian** if $A^\dagger = A$. Two fundamental consequences follow immediately.

1. **Real eigenvalues.** If $A|a\rangle = a|a\rangle$, then $a \in \mathbb{R}$.
   *Proof:* $a\langle a|a\rangle = \langle a|A|a\rangle = \langle A^\dagger a|a\rangle = a^*\langle a|a\rangle$, hence $a = a^*$.
2. **Orthogonal eigenstates.** Eigenstates with distinct eigenvalues are orthogonal: $\langle a_1|a_2\rangle = 0$ whenever $a_1 \neq a_2$.

These properties are exactly what EMTS requires: observable quantities (mass, energy) must be real numbers, and distinct physical configurations must be distinguishable.

### 4.3.1 Spectral decomposition

For a Hermitian operator $A$ with eigenvalues $\{a_k\}$ and rank-1 projectors $P_k = |a_k\rangle\langle a_k|$, the **spectral theorem** guarantees

$$A = \sum_k a_k P_k, \qquad \sum_k P_k = \mathbf{1}, \qquad P_j P_k = \delta_{jk} P_k.$$

This decomposition bridges abstract operator algebra to physical measurement: each term $a_k P_k$ pairs a possible measurement outcome $a_k$ with the projector that selects it from any state. Given a state $|\psi\rangle$, the Born rule states that outcome $a_k$ is obtained with probability

$$\mathbb{P}(a_k) = \langle\psi|P_k|\psi\rangle,$$

and the post-measurement state is

$$\frac{P_k|\psi\rangle}{\sqrt{\mathbb{P}(a_k)}}.$$

## 4.4 The Mass Operator

The observable corresponding to the *mass component* of an EMTS state is

$$\hat{M} = |m\rangle\langle m| = \begin{pmatrix} 1 & 0 \\ 0 & 0 \end{pmatrix}.$$

This is the Hermitian projector onto the mass basis vector. Its spectral decomposition has eigenvalues $\{1, 0\}$:

$$\hat{M}|m\rangle = 1 \cdot |m\rangle, \tag{4.1}$$

$$\hat{M}|E\rangle = 0 \cdot |E\rangle. \tag{4.2}$$

### 4.4.1 Measurement probability

For the EMTS state $|\psi\rangle = \cos\theta\,|m\rangle + i\sin\theta\,|E\rangle$, the Born rule gives

$$\mathbb{P}(m) = \langle\psi|\hat{M}|\psi\rangle = \langle\psi|m\rangle\langle m|\psi\rangle = |\cos\theta|^2 = \cos^2\theta.$$

This is the quantum-mechanical expression of the EMTS **projection principle** (Section 2.2.2): the probability of observing mass equals the square of the real projection $\cos\theta$, precisely as the geometric observable $\Re(z) = r\cos\theta$ suggested.

### 4.4.2 Post-measurement state

Upon obtaining outcome $m = 1$, the state collapses to

$$\frac{\hat{M}|\psi\rangle}{\sqrt{\mathbb{P}(m)}} = \frac{\cos\theta\,|m\rangle}{|\cos\theta|} = |m\rangle.$$

The imaginary energy component vanishes from the observable record—the system has been "projected to the real axis," in perfect correspondence with the EMTS measurement picture.

## 4.5 The Energy Operator

Symmetrically, the *energy component* is described by

$$\hat{E}_{\text{obs}} = |E\rangle\langle E| = \begin{pmatrix} 0 & 0 \\ 0 & 1 \end{pmatrix},$$

with measurement probability

$$\mathbb{P}(E) = \langle\psi|\hat{E}_{\text{obs}}|\psi\rangle = \sin^2\theta.$$

Note that

$$\mathbb{P}(m) + \mathbb{P}(E) = \cos^2\theta + \sin^2\theta = 1,$$

confirming that $\{\hat{M}, \hat{E}_{\text{obs}}\}$ form a *complete*, exhaustive pair of projectors: the system must register in one or the other when measured. The EMTS parameter $\theta$ therefore encodes the *relative probability* of finding the system in its mass-like versus energy-like configuration.

## 4.6 The EMTS Hamiltonian and Time Evolution

In EMTS, the phase advances linearly as $\theta = \omega t$. This continuous rotation in the $\{|m\rangle, |E\rangle\}$ plane is generated by a Hermitian Hamiltonian. The natural generator of the infinitesimal transformation

$$\cos\theta \;\to\; \cos(\theta + d\theta), \qquad \sin\theta \;\to\; \sin(\theta + d\theta)$$

in $\mathcal{H}$ is

$$\hat{H} = \frac{\hbar\omega}{2}\,\sigma_y = \frac{\hbar\omega}{2}\begin{pmatrix} 0 & -i \\ i & 0 \end{pmatrix},$$

where $\sigma_y$ is the Pauli $y$-matrix. This operator is Hermitian ($\sigma_y^\dagger = \sigma_y$) with eigenvalues $\pm\hbar\omega/2$.

### 4.6.1 Schrödinger equation in EMTS

Unitary time evolution is given by

$$|\psi(t)\rangle = U(t)|\psi(0)\rangle, \qquad U(t) = e^{-i\hat{H}t/\hbar} = e^{-i\omega t\,\sigma_y/2}.$$

Evaluating the matrix exponential via sin and cos:

$$U(t) = \begin{pmatrix} \cos\frac{\omega t}{2} & -\sin\frac{\omega t}{2} \\ \sin\frac{\omega t}{2} & \cos\frac{\omega t}{2} \end{pmatrix}.$$

Starting from the mass eigenstate $|\psi(0)\rangle = |m\rangle$:

$$|\psi(t)\rangle = \cos\left(\frac{\omega t}{2}\right)|m\rangle + \sin\left(\frac{\omega t}{2}\right)|E\rangle.$$

With $\theta \equiv \omega t/2$ this recovers the canonical EMTS state, and the mass measurement probability oscillates as[4]

$$\mathbb{P}(m, t) = \cos^2\left(\frac{\omega t}{2}\right),$$

which is the quantum manifestation of the projection $m(t) = r\cos(\omega t)$ in the classical EMTS picture.

### 4.6.2 Energy eigenvalues and EMTS phase quadrants

The eigenvalues $\pm\hbar\omega/2$ of $\hat{H}$ correspond to the two stationary states. In the EMTS geometric picture these map to $\theta = 0$ (mass-dominated, $Q_{\text{I}}$ regime) and $\theta = \pi$ (anti-mass, $Q_{\text{III}}$ regime). Time evolution continuously sweeps through all four force quadrants, as summarised in Table 4.1.

| Phase window | Quadrant | $\mathbb{P}(m)$ | Character | Force |
|---|---|---|---|---|
| $\theta = 0$ | real$^+$ axis | $= 1$ | Pure mass (rest) | — (graviton/photon pole) |
| $\theta \in (0,\, \pi/2)$ | $Q_{\mathrm{I}}$ | $> 1/2$ | Mass-dominated | Electromagnetic |
| $\theta = \pi/2$ | imag$^+$ axis | $= 0$ | Pure energy | photon pole |
| $\theta \in (\pi/2,\, \pi)$ | $Q_{\mathrm{II}}$ | $< 1/2$ | Energy-dominated | Weak nuclear |
| $\theta = \pi$ | real$^-$ axis | $= 1$ | Anti-mass | $CP$ boundary |
| $\theta \in (\pi,\, 3\pi/2)$ | $Q_{\mathrm{III}}$ | $< 1/2$ | Both components $< 0$ | Strong nuclear |
| $\theta = 3\pi/2$ | imag$^-$ axis | $= 0$ | Negative energy | vacuum/Casimir |
| $\theta \in (3\pi/2,\, 2\pi)$ | $Q_{\mathrm{IV}}$ | $> 1/2$ | Mass$^+$, energy$^-$ | Gravitational |

Table 4.1: Mass measurement probability $\mathbb{P}(m) = \cos^2\theta$ across all EMTS phase regions. Boundary axes ($\theta = 0, \pi/2, \pi, 3\pi/2$) are force-transition interfaces that host the massless mediators; see Chapter 5.

## 4.7 Commutator Structure and the Uncertainty Principle

Two observables $A$ and $B$ are **compatible** (simultaneously measurable) if and only if $[A, B] = AB - BA = 0$. For the EMTS projectors:

$$[\hat{M}, \hat{E}_{\mathrm{obs}}] = |m\rangle\langle m|E\rangle\langle E| - |E\rangle\langle E|m\rangle\langle m| = 0,$$

since $\langle m|E\rangle = 0$. The mass and energy projectors *commute*: they share the common eigenbasis $\{|m\rangle, |E\rangle\}$ and are simultaneously diagonalizable. Measuring one does not disturb the other.

However, the mass operator $\hat{M}$ and the Hamiltonian $\hat{H}$ do *not* commute:

$$[\hat{M}, \hat{H}] = \frac{\hbar\omega}{2}(\hat{M}\sigma_y - \sigma_y\hat{M}) = \frac{i\hbar\omega}{2}\begin{pmatrix} 0 & 1 \\ -1 & 0 \end{pmatrix} \neq 0.$$

This non-commutativity encodes the core EMTS dynamical principle: *a state with definite mass has indefinite energy, and vice versa.* The Robertson uncertainty relation

$$\Delta M \cdot \Delta H \;\geq\; \frac{1}{2}\big|\langle[\hat{M}, \hat{H}]\rangle\big|$$

quantifies this trade-off, directly paralleling the classical EMTS circle identity $(m/r)^2 + (E/r)^2 = 1$: fixing one component forces uncertainty in the other.

## 4.8 Expectation Values and the EMTS Observable

The **expectation value** of an observable $A$ in state $|\psi\rangle$ is

$$\langle A\rangle_\psi = \langle\psi|A|\psi\rangle \in \mathbb{R}.$$

Hermiticity guarantees this is real. For the canonical EMTS state:

$$\langle\hat{M}\rangle = \cos^2\theta, \tag{4.3}$$

$$\langle\hat{E}_{\mathrm{obs}}\rangle = \sin^2\theta, \tag{4.4}$$

$$\langle\hat{H}\rangle = -\frac{\hbar\omega}{2}\cos(2\theta). \tag{4.5}$$

The expectation value $\langle\hat{M}\rangle = \cos^2\theta$ is the quantum-mechanical analogue of the EMTS projection $\Re(z)/r = \cos\theta$, lifted from a purely geometric ratio to a measurable probability. The full modulus $r$ supplements this picture by setting the energy-mass scale: the observable "real" value is $r\langle\hat{M}\rangle^{1/2} = r|\cos\theta|$.

## 4.9 Summary

This chapter has established the following:

1. The EMTS state space is the Hilbert space $\mathcal{H} = \mathbb{C}^2$ with mass-energy basis $\{|m\rangle, |E\rangle\}$.
2. Hermitian operators are the *correct* mathematical objects for EMTS observables: their real eigenvalues guarantee real measurement outcomes, and their orthogonal eigenstates mirror the EMTS mass-energy split.
3. The mass operator $\hat{M}$ makes the EMTS projection principle precise: $\mathbb{P}(m) = \cos^2\theta$ is the probability of finding the system on the real axis at phase $\theta$.
4. The Hamiltonian $\hat{H} = \frac{\hbar\omega}{2}\sigma_y$ drives the rotation $\theta = \omega t$, generating all EMTS dynamics from a single Hermitian generator.
5. Non-commutativity $[\hat{M}, \hat{H}] \neq 0$ enforces the mass-energy uncertainty that is geometrically encoded in the circular identity $m^2 + E^2 = r^2$.

With these operator-theoretic foundations in place, the next chapter examines how EMTS states couple to the fundamental forces and how the standard-model interactions emerge from the phase structure of the complex plane.

# Chapter 5

# The Quadrants and Their Implications

The EMTS framework assigns a physical meaning not just to the magnitude $r$ and the phase $\theta$ of the complex state $z = m + iE = re^{i\theta}$, but to the *quadrant* in which the state resides at the moment of interaction. The central hypothesis of this chapter is:

> **Force-tagging postulate.** The interaction channel observed in spacetime is tagged by the quadrant of the pre-collapse state $z(t_0) = re^{i\theta_0}$. Each of the four fundamental forces is the dominant interaction mode for states residing in the corresponding quarter of the complex $m$–$E$ plane.

This is not merely a labelling convenience. The signs of $m = r\cos\theta_0$ and $E = r\sin\theta_0$ encode qualitatively different physical regimes—positive vs. negative effective mass, absorptive vs. emissive energy—and each regime selects a different symmetry group and mediating boson family.

## 5.1 Phase Windows as Hermitian Projectors

The mathematical object that carves out a quadrant is a **phase-window projector**. Define the indicator function for force $f$:

$$W_f(\theta) = \begin{cases} 1, & \theta \in \Delta_f, \\ 0, & \text{otherwise}, \end{cases}$$

where $\Delta_f$ is the phase interval assigned to force $f$ (Table 5.1). A smooth, physical version replaces the step function with a squared cosine bell

$$\tilde{W}_f(\theta) = \cos^2\!\left(\frac{\theta - \theta_f^{\text{mid}}}{\Delta\theta_f}\,\frac{\pi}{2}\right) \cdot \mathbf{1}_{\theta\in\Delta_f}$$

that tapers to zero at the quadrant boundaries, avoiding divergences in the coupling integral. Coupling strength at scale $r$ is then the cycle average

$$\bar{g}_f(r) = \frac{\omega(r)}{2\pi}\int_0^{2\pi} W_f(\theta)\, g_f(\theta, r)\, d\theta,$$

where $g_f(\theta, r)$ is a force-specific coupling function discussed in each subsection below. In the Hilbert-space language of Chapter 4, $W_f$ acts as a Hermitian projector onto the subspace of states whose phase lies in $\Delta_f$, and $\bar{g}_f$ is the expectation value of the coupling operator in that subspace.

| Quadrant | Force | Phase window $\Delta_f$ | sgn($m$) | sgn($E$) | Mediator |
|---|---|---|---|---|---|
| $Q_{\mathrm{I}}$ | Electromagnetic | $\left(0,\ \frac{\pi}{2}\right)$ | + | + | Photon $\gamma$ |
| $Q_{\mathrm{II}}$ | Weak nuclear | $\left(\frac{\pi}{2},\ \pi\right)$ | − | + | $W^{\pm}$, $Z^0$ |
| $Q_{\mathrm{III}}$ | Strong nuclear | $\left(\pi,\ \frac{3\pi}{2}\right)$ | − | − | Gluons $g$ |
| $Q_{\mathrm{IV}}$ | Gravitational | $\left(\frac{3\pi}{2},\ 2\pi\right)$ | + | − | Graviton $G$ |

Table 5.1: Assignment of fundamental forces to phase quadrants of the EMTS complex plane. The signs of the real projection $m = r\cos\theta$ and imaginary component $E = r\sin\theta$ characterise each regime.

## 5.2 Quadrant I — Electromagnetic Force

**Phase window:** $\theta \in (0, \frac{\pi}{2}), \quad m = r\cos\theta > 0, \quad E = r\sin\theta > 0.$

In $Q_{\mathrm{I}}$ the system possesses *positive real mass and positive energy.* This is the most familiar physical regime: a massive, energetic particle propagating with a well-defined positive rest mass.

### Physical character

The electromagnetic force is mediated by the massless photon, which corresponds to the *boundary* $\theta = \pi/2$ of $Q_{\mathrm{I}}$—the pure-imaginary axis where $m = 0$ and the state carries only energy. Because the mediator lives on the quadrant boundary, the force is infinite-ranged: the photon can transport energy $E = \hbar\omega$ across arbitrarily large distances without a mass penalty.

Within $Q_{\mathrm{I}}$, the coupling function is approximately

$$g_{\mathrm{EM}}(\theta, r) \approx \frac{\alpha}{r}\cos^2\theta, \qquad \alpha \approx \frac{1}{137},$$

where $\alpha$ is the fine-structure constant. The $\cos^2\theta$ factor reflects the projection principle: only the mass component $m/r = \cos\theta$ couples to the electromagnetic field. Purely energetic states ($\theta \to \pi/2$) carry less charge and interact more weakly, while purely massive states ($\theta \to 0$) couple most strongly.

### Symmetry in EMTS

The gauge symmetry of electromagnetism, $U(1)$, corresponds to a global phase shift $\theta \mapsto \theta + \alpha$ that leaves $r$ unchanged. In the Hilbert-space representation this is the unitary operator $U(\alpha) = e^{i\alpha\hat{N}}$, where $\hat{N} = |E\rangle\langle E| - |m\rangle\langle m|$ counts the energy-to-mass imbalance. Electromagnetic interactions are thus phase rotations that keep the system within (or near) $Q_{\mathrm{I}}$.

## 5.3 Quadrant II — Weak Nuclear Force

**Phase window:** $\theta \in (\frac{\pi}{2}, \pi), \quad m = r\cos\theta < 0, \quad E = r\sin\theta > 0.$

In $Q_{\mathrm{II}}$ the real projection $m$ is *negative* while the energy component remains positive. Negative $m$ does not imply a physical anti-particle; rather, it signals that the state has crossed the pure-energy axis and the observable on the real axis now points in the negative direction—it is an *inverted mass configuration.*

### Physical character

The weak force is mediated by the massive $W^{\pm}$ and $Z^0$ bosons. Their masses ($m_W \approx 80$ GeV, $m_Z \approx 91$ GeV) arise because the mediators *must* cross from the $Q_{\mathrm{II}}$ regime back toward the real axis to transmit the interaction, paying a mass penalty encoded by the crossing distance $|\theta - \pi/2|$. This gives the weak force its characteristically short range,

$$\lambda_{\mathrm{weak}} \sim \frac{\hbar c}{m_W c^2} \approx 2 \times 10^{-18}\ \mathrm{m}.$$

### Flavour mixing and the EMTS picture

A hallmark of the weak force is **flavour mixing**: it transforms one quark or lepton flavour into another. In EMTS terms, a weak interaction shifts the phase $\theta$ discontinuously across the $Q_{\mathrm{I}}$–$Q_{\mathrm{II}}$ boundary ($\theta = \pi/2$), moving the state from a positive-mass to a negative-mass configuration and back. This boundary transition corresponds to a *parity flip* ($m \to -m$), naturally explaining why the weak force is the only interaction that violates parity ($P$) symmetry—it is the only force whose mediator must cross the imaginary axis.

The coupling function is approximately

$$g_{\mathrm{W}}(\theta, r) \approx \frac{g_2^2}{r}\, e^{-m_W r/\hbar c}\, |\cos\theta|,$$

where $g_2$ is the weak coupling constant and the exponential Yukawa suppression reflects the massive mediator.

## 5.4 Quadrant III — Strong Nuclear Force

**Phase window:** $\theta \in \left(\pi, \frac{3\pi}{2}\right), \quad m = r\cos\theta < 0, \quad E = r\sin\theta < 0.$

$Q_{\mathrm{III}}$ is the only quadrant where *both* components are negative. This doubly-inverted regime corresponds to states deep inside nuclear scales, where both the observable mass projection and the energy carrying capacity point opposite to the macroscopic conventions.

### Physical character

The strong force is mediated by eight massless gluons and governs quark confinement. Its key distinguishing feature is **asymptotic freedom** and **confinement**:

- **Asymptotic freedom** ($r \to 0$): At short distances the coupling weakens. In EMTS, small $r$ means the state has low modulus (low mass-energy), and both negative components are small in magnitude—the state barely occupies $Q_{\mathrm{III}}$ and couples weakly.
- **Confinement** ($r \to \infty$): As $r$ grows, states deep in $Q_{\mathrm{III}}$ cannot close their EMTS orbit into a real projection. The coupling grows linearly:

  $$g_{\mathrm{S}}(\theta, r) \approx \alpha_s(r)\, r, \qquad \alpha_s(r) \sim \frac{1}{\ln(r_0/r)},$$

  producing a flux tube of rising potential that prevents isolated quarks from appearing as free observable particles.

### Colour charge and SU(3)

The three colour charges (red, green, blue) correspond to three independent phase orientations within $Q_{\mathrm{III}}$, each separated by $2\pi/3$. Only colour-neutral combinations—states whose joint phase averages to $\pi$ (the midpoint of $Q_{\mathrm{III}}$, i.e., on the negative real axis)—produce closed EMTS orbits that project to a real, observable hadron. This is the EMTS geometric interpretation of $SU(3)$ colour neutrality.

## 5.5 Quadrant IV — Gravitational Force

**Phase window:** $\theta \in \left(\frac{3\pi}{2}, 2\pi\right), \quad m = r\cos\theta > 0, \quad E = r\sin\theta < 0.$

In $Q_{\mathrm{IV}}$ the mass projection is again positive—as in $Q_{\mathrm{I}}$—but the energy component is *negative*. A negative imaginary component means the state is decelerating, emitting energy, or losing phase coherence: the hallmarks of gravitational attraction and energy dissipation.

### Physical character

Gravity is the weakest force at particle scales but the only one that is always attractive and infinite-ranged. Its mediator, the graviton $G$, is conjectured to be massless (like the photon), and it lives on the $Q_{\mathrm{IV}}$–$Q_{\mathrm{I}}$ boundary at $\theta = 0$ (or equivalently $2\pi$)—the positive real axis, where pure mass and zero energy meet.

The coupling function is

$$g_{\mathrm{G}}(\theta, r) \approx \frac{G_N\, r^2}{r_{\mathrm{P}}^2}\, \cos^2\theta, \qquad r_{\mathrm{P}} = \sqrt{\frac{\hbar G_N}{c^3}} \approx 1.6 \times 10^{-35}\ \mathrm{m},$$

where $G_N$ is Newton's constant and $r_{\mathrm{P}}$ is the Planck length. The $\cos^2\theta$ factor is the same as in electromagnetism—both forces couple to the mass projection—but the scale factor $r^2/r_{\mathrm{P}}^2$ suppresses gravity enormously at sub-Planckian radii, explaining the hierarchy problem geometrically: gravity is weak because the Planck length is tiny compared to every other scale in the theory.

### Always attractive

In $Q_{\mathrm{IV}}$ we have $E < 0$, meaning the state is losing energy to the field. Since the force is proportional to $-\partial g_{\mathrm{G}}/\partial r \propto -G_N m_1 m_2/r^2$ (always negative, i.e., attractive), gravity never repels. There is no quadrant analogous to the electromagnetic case where $E > 0$ states could push back, so the force has no repulsive branch. This geometric asymmetry between $Q_{\mathrm{I}}$ and $Q_{\mathrm{IV}}$ is the EMTS explanation for why gravity cannot be screened.

## 5.6 Boundary Axes as Transition Zones

The four quadrant boundaries (the coordinate axes of the $m$–$E$ plane) are physically significant in their own right:

| Axis | Condition | State type | Physical role |
|---|---|---|---|
| $\theta = 0$ | $m > 0,\ E = 0$ | Pure mass (rest) | Classical matter; graviton pole |
| $\theta = \pi/2$ | $m = 0,\ E > 0$ | Pure energy | Massless bosons; photon pole |
| $\theta = \pi$ | $m < 0,\ E = 0$ | Anti-mass | Antimatter boundary; $CP$ axis |
| $\theta = 3\pi/2$ | $m = 0,\ E < 0$ | Negative energy | Vacuum fluctuations; Casimir states |

States sitting exactly on an axis are eigenstates of either $\hat{M}$ or $\hat{E}_{\text{obs}}$ (Chapter 4), and the axes themselves act as *force-transition interfaces*. A particle undergoing a phase transition from one quadrant to another must necessarily pass through one of these axes, which is why interactions at the quadrant boundaries are associated with the emission or absorption of the corresponding massless (boundary-resident) mediator.

## 5.7 Force Hierarchy from Phase Geometry

A qualitative but illuminating observation emerges when the four cycle-averaged coupling strengths are compared as a function of $r$. Each $\bar{g}_f(r)$ inherits a different $r$-dependence from the structure of its quadrant:

| Force | $r$-scaling of $\bar{g}_f$ | Observed range |
|---|---|---|
| Strong | $\sim \alpha_s(r) \cdot r$ | $\lesssim 10^{-15}$ m (grows then confines) |
| Electromagnetic | $\sim \alpha/r$ | $\infty$ (power-law) |
| Weak | $\sim g_2^2 e^{-m_W r}/r$ | $\sim 10^{-18}$ m (Yukawa) |
| Gravitational | $\sim G_N r^2/r_{\text{P}}^2$ | $\infty$ (power-law, tiny $G_N$) |

At the scale of everyday matter ($r \sim r_{\text{Bohr}} \approx 0.5$ Å), the hierarchy $\alpha_s \gg \alpha \gg g_2^2 e^{-m_W r} \gg G_N/r_{\text{P}}^2 r^{-2}$ is entirely consistent with the standard measured values. The EMTS quadrant model does not derive these numerical values from first principles, but it *organises* them into a coherent geometric structure: forces become arrayed in the complex plane not by coincidence but because each quadrant imposes different sign constraints and range behaviours on the coupling integral.

## 5.8 Is the Four-Fold Coincidence Real?

A natural—and important—question arises at this point:

*Is it a coincidence that there are four fundamental forces and four quadrants?*

The short answer, within the EMTS framework, is **no**. But the reasoning deserves care, because the same count "four" carries different epistemic weights on each side of the equation.

### Why four quadrants is inevitable

The complex plane $\mathbb{C}$ has two real coordinates, $m$ and $E$, each of which can be positive or negative. The number of sign combinations is

$$|\{+, -\}|^2 = 2^2 = 4.$$

This is not a hypothesis about physics—it is an arithmetic fact about the dimensionality of the representation space. Given the EMTS postulate that physical states are complex numbers $z = m + iE$, *there could not be any other number of quadrants.*

More formally, the symmetry group that permutes sign combinations is the Klein four-group $V_4 \cong \mathbb{Z}_2 \times \mathbb{Z}_2$, generated by the two independent reflections

$$\sigma_m : m \mapsto -m \quad \text{(mass parity)}, \qquad \sigma_E : E \mapsto -E \quad \text{(energy parity)}.$$

The four quadrants are exactly the four orbits of $V_4$ acting on the non-zero points of $\mathbb{C} \setminus \{0\}$. Any two-dimensional real representation of a physical state will have this fourfold orbit structure.

### Why four forces is *not* fundamental

From the standard-physics side, the count "four" is historically and energetically contingent:

- **Electroweak unification** (Glashow–Salam–Weinberg, 1960s–70s): at energies above $\sim 100$ GeV the electromagnetic and weak forces merge into a single $SU(2)_L \times U(1)_Y$ interaction. The apparent split into two forces at low energies arises from spontaneous symmetry breaking (the Higgs mechanism), which gives the $W^{\pm}$ and $Z^0$ bosons their masses and leaves the photon massless. If one works above the electroweak scale, there are effectively *three* forces, not four.
- **Grand Unified Theories (GUTs)** predict a further merger of the electroweak and strong forces into a single $SU(5)$ (or larger) gauge group at energies $\sim 10^{15}$ GeV, reducing the count to *two*: a single unified force plus gravity.
- **String/M-theory** candidates suggest all four may be facets of a single eleven-dimensional geometric structure, making the count *one*.

So the number four is a low-energy, broken-symmetry artefact of the Standard Model, not a Platonic constant of nature.

### The EMTS interpretation

Putting both sides together, the EMTS perspective is the following:

1. The complex plane *necessarily* produces exactly four sign-distinct regimes.
2. Nature at low energies *empirically* exhibits four dominant interaction channels.
3. The EMTS framework is a mapping of the low-energy effective theory: it assigns each empirically observed force to the quadrant whose sign structure best matches the force's qualitative properties (range, attractive vs. repulsive, mass-dependent vs. charge-dependent coupling).

The match between four quadrants and four forces is therefore a *necessary* consequence of EMTS applied to the low-energy Standard Model, not a numerical coincidence. The deeper question—whether the fourfold structure of the complex plane is the *reason* nature exhibits (approximately) four forces at low energies, or merely a convenient coordinate system for describing them—remains a topic of ongoing investigation in the theoretical framework.

#### Higher-energy modifications

If the electroweak unification is taken seriously within EMTS, then above the electroweak scale the $Q_{\mathrm{I}}$ and $Q_{\mathrm{II}}$ quadrants must *merge*. This would correspond to the phase boundary at $\theta = \pi/2$ becoming dynamical: the imaginary axis ceases to be a sharp dividing wall between EM and Weak regimes and instead becomes a transition band of width $\sim \hbar/m_W c$ that widens as energy increases. At GUT scales, three quadrants merge further, and one would work with an effective single-quadrant covering almost the entire upper half-plane $\{\theta \in (0, \pi)\}$. The geometrical language survives high-energy unification; only the sharpness of the quadrant boundaries changes.

## 5.9 Quadrant Transitions: Speculation on Induced Force-Channel Switching

*What happens if a system is driven from one quadrant to another?*

Under natural evolution the phase $\theta(t) = \omega t$ advances continuously, so a freely evolving EMTS state sweeps through all four quadrants in one period $T = 2\pi/\omega$. This is ordinary, unforced dynamics. The interesting question is what it would mean to *engineer* a transition—to apply an external perturbation that moves the state from its natural quadrant into a different one, changing its dominant interaction channel.

### 5.9.1 Boundary crossings and their cost

Each quadrant boundary is a specific coordinate axis of the $m$–$E$ plane. Crossing it requires passing through a qualitatively special intermediate state:

| Boundary | Condition at crossing | Intermediate state | Energy cost |
|---|---|---|---|
| $\theta = \pi/2$ | $m = 0,\ E > 0$ | Momentarily massless, energetic | $\Delta E \sim m_W c^2 \approx 80$ GeV |
| $\theta = \pi$ | $m < 0,\ E = 0$ | Anti-mass, zero energy | $\Delta E \sim \Lambda_{\mathrm{QCD}} \approx 200$ MeV |
| $\theta = 3\pi/2$ | $m = 0,\ E < 0$ | Massless, negative energy | $\Delta E \sim E_{\mathrm{P}} = \sqrt{\hbar c^5/G_N}$ (Planc |
| $\theta = 0\,(2\pi)$ | $m > 0,\ E = 0$ | Pure rest mass, zero kinetic energy | $\Delta E \sim 0$ (free, any mass) |

The $\theta = 3\pi/2$ crossing (entering or leaving $Q_{\mathrm{IV}}$) demands a Planck-scale energy to sustain a massless, negative-energy intermediate state—which is why the gravitational force is not only weak but effectively *non-switchable* at any energy accessible today. The $\theta = 0$ boundary, by contrast, is free: a particle at rest with positive mass naturally sits there, and the cost of slightly perturbing $\theta$ away from zero is $O(\omega)$—achievable with any nonzero energy input.

### 5.9.2 The six transitions: a taxonomy

There are six distinct pairs of quadrants: four *adjacent* (sharing a boundary axis) and two *diagonal* (no shared boundary). Table 5.2 catalogues them.

### 5.9.3 Adjacent transitions in known physics

Several standard processes can be re-read as quadrant transitions.

| Transition | Axis crossed | Sign change | Physical interpretation | K |
|---|---|---|---|---|
| $Q_{\mathrm{I}} \to Q_{\mathrm{II}}$ | $\theta = \pi/2$ | $m : + \to -$ | Mass becomes anti-mass; parity flip | $\beta$- |
| $Q_{\mathrm{II}} \to Q_{\mathrm{III}}$ | $\theta = \pi$ | $E : + \to -$ | Energy-absorbing becomes energy-emitting | |
| $Q_{\mathrm{III}} \to Q_{\mathrm{IV}}$ | $\theta = 3\pi/2$ | $m : - \to +$ | Confinement released into gravity | |
| $Q_{\mathrm{IV}} \to Q_{\mathrm{I}}$ | $\theta = 0$ | $E : - \to +$ | Gravitational decay into EM radiation | H |
| $Q_{\mathrm{I}} \leftrightarrow Q_{\mathrm{III}}$ | $\pi/2$ then $\pi$ | $m, E$ both flip | Full sign inversion; matter↔anti-matter+confinement | Anni |
| $Q_{\mathrm{II}} \leftrightarrow Q_{\mathrm{IV}}$ | $\pi$ then $3\pi/2$ | $m, E$ both flip | Weak-sector anti-mass in gravitational collapse | |

Table 5.2: All six quadrant-pair transitions, the boundary axis crossed, the sign that flips, and the closest known physical process.

**$Q_{\mathrm{I}} \to Q_{\mathrm{II}}$ (crossing $\theta = \pi/2$): Beta decay.** In neutron beta decay, $n \to p + e^- + \bar{\nu}_e$, a down quark in the Strong/EM regime acquires a $W^-$ vertex. In EMTS terms the quark's phase is pushed across $\theta = \pi/2$: $m$ briefly vanishes (massless intermediate state mediated by $W^-$) and then re-emerges negative. The proton is a composite that re-establishes a positive-$m$ projection by redistributing phase among its three quarks, while the electron carries the crossed-phase information out as an observable particle. The parity violation observed in weak decays is, in this picture, the direct signature of $m$ changing sign—the observable projection $\Re(z)$ reverses under the crossing.

**$Q_{\mathrm{IV}} \to Q_{\mathrm{I}}$ (crossing $\theta = 0$): Hawking radiation.** A black hole's gravitational field corresponds to states deep in $Q_{\mathrm{IV}}$ ($m > 0$, $E < 0$, emitting energy inward). Hawking's calculation shows that quantum fluctuations at the event horizon produce photons that escape to infinity. In EMTS this is a *boundary crossing at* $\theta = 0$: a virtual pair is produced straddling the positive real axis, one partner falls deeper into $Q_{\mathrm{IV}}$ (absorbed by the black hole) and the other crosses into $Q_{\mathrm{I}}$ ($E > 0$) and propagates away as a real photon. The boundary $\theta = 0$ is the cheapest crossing (zero rest-mass cost), which is consistent with Hawking radiation being a low-energy, thermal process relative to the Planck scale.

**$Q_{\mathrm{II}} \to Q_{\mathrm{III}}$ (crossing $\theta = \pi$): Hadronisation.** After a high-energy weak collision produces free quarks, the strong force reasserts itself and the quarks hadronise—forming bound states. In EMTS the quarks, briefly in $Q_{\mathrm{II}}$ (high-energy, $E > 0$, $m < 0$), lose energy through gluon radiation and their phase rotates through $\theta = \pi$ (the negative real axis, $E \to 0$ then $E < 0$), settling into the confining $Q_{\mathrm{III}}$ regime. The $\Lambda_{\mathrm{QCD}}$ energy scale of the boundary crossing matches the observed hadronisation energy scale $\sim 200$ MeV.

### 5.9.4 Diagonal transitions: simultaneous sign flips

Diagonal transitions flip *both* $\mathrm{sgn}(m)$ and $\mathrm{sgn}(E)$ simultaneously. In the operator language of Chapter 4, the state passes through the origin $z = 0$—a singularity of undefined phase. There are two diagonal pairs:

**$Q_{\mathrm{I}} \leftrightarrow Q_{\mathrm{III}}$.** Both components flip: $m \to -m$, $E \to -E$. This is precisely the action of the combined parity-times-time-reversal operator $PT$, which in quantum field theory maps a particle to its *CPT conjugate*. If $Q_{\mathrm{I}}$ hosts ordinary matter (positive mass, positive energy propagating forward in time) then $Q_{\mathrm{III}}$ contains, in this interpretation, a shadow regime that is simultaneously anti-massed and time-reversed. The process $e^+ + e^- \to \gamma\gamma$ (pair annihilation) can be read as the electron ($z \in Q_{\mathrm{I}}$) and positron ($z \in Q_{\mathrm{III}}$ by $PT$ symmetry) annihilating at $z = 0$ and re-emerging as photons on the $\theta = \pi/2$ boundary.

**$Q_{\mathrm{II}} \leftrightarrow Q_{\mathrm{IV}}$.** The other diagonal pair maps Weak states ($m < 0$, $E > 0$) to Gravitational states ($m > 0$, $E < 0$). This is speculative territory: no known process unambiguously transitions between the weak and gravitational regimes. However, in the early universe at temperatures above the electroweak scale, weak and gravitational interactions were comparably strong. An EMTS perspective would suggest that at those energies the $Q_{\mathrm{II}}$–$Q_{\mathrm{IV}}$ boundary becomes traversable—potentially observable as an asymmetry between gravitational and weak contributions to the stress-energy tensor in primordial cosmology.

### 5.9.5 Induced transitions: what would it take?

Assuming we could engineer an external field that selectively shifts $\theta$, what would "force-channel switching" require in practice?

The transition operator that maps $Q_{\mathrm{I}}$ into $Q_{\mathrm{II}}$ is $\sigma_m$, the mass parity operator:

$$\sigma_m = |m\rangle\langle m| - |E\rangle\langle E| = \begin{pmatrix} 1 & 0 \\ 0 & -1 \end{pmatrix} = \sigma_z.$$

Applied to the canonical EMTS state $|\psi\rangle = \cos\theta|m\rangle + i\sin\theta|E\rangle$, this gives $\sigma_m|\psi\rangle = \cos\theta|m\rangle - i\sin\theta|E\rangle$, which is the state at phase $-\theta$ — a time-reversal in the EMTS picture. The analogous energy parity, $\sigma_E = \sigma_x$ in the EMTS basis, reflects across the real axis ($E \to -E$), mapping $Q_{\mathrm{I}}$ to $Q_{\mathrm{IV}}$ and $Q_{\mathrm{II}}$ to $Q_{\mathrm{III}}$. Their product

$$\sigma_m\sigma_E = \begin{pmatrix} 0 & 1 \\ -1 & 0 \end{pmatrix}$$

performs the diagonal flip and corresponds to rotating by $\pi$ in the Hilbert space.

The practical requirement for each induced transition is therefore a Hamiltonian perturbation $\delta\hat{H}$ that is *off-diagonal* in the $\{|m\rangle, |E\rangle\}$ basis — precisely the weak-force interaction Hamiltonian in the Standard Model. This is not surprising: the purpose of the $W^{\pm}$ bosons is exactly to move states across the mass-sign boundary.

| **Induced transition** | **Required operator** | **Analogy** |
|---|---|---|
| $Q_{\mathrm{I}} \to Q_{\mathrm{II}}$ | $\sigma_m = \sigma_z$ | $W^{\pm}$ vertex; parity-flip |
| $Q_{\mathrm{I}} \to Q_{\mathrm{IV}}$ | $\sigma_E = \sigma_x$ | Gravitational redshift; photon blue/redshift |
| $Q_{\mathrm{I}} \to Q_{\mathrm{III}}$ | $\sigma_m\sigma_E$ | Annihilation into gluons; QCD vacuum |

### 5.9.6 Speculative implications

Taking the quadrant-transition picture seriously leads to several speculative but internally consistent hypotheses.

**Force transmutation.** If a macroscopic object could be driven into $Q_{\mathrm{III}}$ en masse — its constituent particles' phases all shifted past $\theta = \pi$ simultaneously — the dominant interaction would switch from electromagnetic to strong. The object would "colour up": its atoms would no longer interact electromagnetically but would instead experience the short-range, confining strong force. This is obviously prevented by the $\sim 80$ GeV per-particle cost of crossing $\theta = \pi/2$ first, but it suggests that at sufficiently high temperatures (above the QCD crossover, $T \gtrsim 150$ MeV) dense nuclear matter does indeed transition collectively into a quark-gluon plasma—a state naturally residing in $Q_{\mathrm{III}}$.

**Gravitational-to-electromagnetic phase transition.** The $\theta = 0$ boundary is the cheapest crossing. A speculative implication is that a gravitationally-dominated object (a neutron star or black hole in $Q_{\mathrm{IV}}$) could undergo a spontaneous phase transition into an electromagnetically-dominated state by radiating energy ($E : - \to +$), essentially converting gravitational binding energy into photons. Hawking radiation is a quantum-mechanical trace of this process. A fully classical version may be relevant to the physics of magnetars, whose intense magnetic fields suggest a large electromagnetic component co-existing with extreme gravitational binding.

**A traversable $Q_{\mathbf{III}}$–$Q_{\mathbf{IV}}$ corridor?** The $\theta = 3\pi/2$ boundary normally requires Planck-scale energy. However, if the modulus $r$ is very small — near the Planck length $r_P$ — the energy cost of the crossing scales as $r/r_P$ and becomes of order unity in natural units. This suggests that at the Planck scale, the boundary between the gravitational and strong quadrants is no longer a barrier: states can fluctuate freely between $Q_{\mathrm{III}}$ and $Q_{\mathrm{IV}}$. This is consistent with the popular conjecture that quantum gravity and the strong force unify at the Planck scale, and it provides a geometric EMTS interpretation of that unification: the confinement boundary and the gravitational boundary dissolve into each other when $r \sim r_P$.

**Complete quadrant cycling as a model of particle generation.** If a state sweeps through all four quadrants in a single period $T = 2\pi/\omega$, it experiences each force in sequence. An object that completes $n$ such cycles before being observed will have accumulated a winding number $n$ around the origin. EMTS speculates that this winding number corresponds to the *generation number* of the particle: first generation (electron, up, down) completes one clean cycle; second generation (muon, strange, charm) has a half-integer additional winding from a sub-cycle resonance; third generation (tau, bottom, top) winds twice before closing. This offers a geometric origin for the three-generation structure of the Standard Model — though the quantitative details remain to be worked out.

## 5.10 Summary

The fundamental forces are distributed across the EMTS complex plane as follows:

1. $Q_{\mathbf{I}}$ **(Electromagnetic):** $m > 0$, $E > 0$. Long-range, massless photon mediator on the $Q_{\mathrm{I}}$–$Q_{\mathrm{II}}$ boundary. $U(1)$ phase symmetry. Coupling $\propto \cos^2\theta/r$.

2. $Q_{\mathbf{II}}$ **(Weak):** $m < 0$, $E > 0$. Short-range, massive $W^{\pm}/Z^0$ mediators. Parity-violating because its mediators must cross the imaginary axis. Coupling with Yukawa suppression $e^{-m_W r}$.

3. $Q_{\mathbf{III}}$ **(Strong):** $m < 0$, $E < 0$. Confining, with three colour phases at $2\pi/3$ intervals. Asymptotic freedom at small $r$; linear confinement at large $r$. $SU(3)$ colour neutrality = closed orbit on the negative real axis.

4. $Q_{\mathbf{IV}}$ **(Gravitational):** $m > 0$, $E < 0$. Long-range, purely attractive, massless graviton on the $Q_{\mathrm{IV}}$–$Q_{\mathrm{I}}$ boundary. Always attractive because there is no positive-$E$ branch in $\Delta_{\mathrm{Grav}}$. Coupling suppressed by $(r_{\mathrm{P}}/r)^2$.

The quadrant boundaries (the coordinate axes) act as force-transition interfaces, hosting the massless mediators and governing the conservation laws that apply when a state changes its dominant interaction channel. Chapter 6 builds on this picture by placing Standard Model particles—quarks, leptons, and gauge bosons—explicitly on the complex plane and connecting their properties to the phase structure developed here.

# Part II

# Framework and Mechanics

# Chapter 6

# Standard Model

Building on the EMTS framework (Chapter 2), we map Standard Model particles and forces onto the complex plane. In quantum theory, the state encodes probabilities.[4] In this framework, oscillations with frequency $\omega$ link to detection likelihoods. Particle vs. wave is reconciled: coherent evolution (*wave*) sets channel rates, while projection events (*particles*) are localized outcomes.

## Particle vs. Wave

- **State vector**: carries phase and interferes.
- **Measurement**: projects to outcomes with Born probabilities.
- **Field view**: particles are quantized excitations; waves are coherent field amplitudes.

The cycle-averaged coupling strengths $\bar{g}_f(r)$ are defined via the phase-window integral in Section 5.1 of Chapter 5. Particle-detection rate in channel $f$ is proportional to $\bar{g}_f(r)$; the force-quadrant assignments and $r$-dependence of each coupling are summarised in Section 5.7 of that chapter.

## Quarks in the complex plane

In the EMTS picture we write a generic excitation as $z = m + iE = re^{i\theta}$, with $r$ encoding a space-like scale and $\theta = \omega t$ encoding time-like phase. Quarks can be viewed as excitations whose complex-plane behaviour is constrained by threefold structure:

- **Colour charge** corresponds to how the excitation winds in an internal copy of the complex plane, with three preferred phase orientations ("red, green, blue") in an $SU(3)$-like subspace.
- **Confinement** arises because a single quark's complex trajectory cannot close in the observable $m$–$E$ plane; only colour-neutral combinations lead to closed orbits and stable projections.
- **Flavour** (up, down, strange, etc.) is tied to distinct radii $r$ and characteristic angular frequencies $\omega$, leading to different effective masses and couplings.

In this view, quarks occupy specific bands in $r$ and families of allowed phase patterns in $\theta$, with hadrons emerging as composite closed paths whose joint projection appears as a single particle.

## Leptons as simpler orbits

Leptons lack colour charge and so correspond to simpler trajectories on the same complex plane. Their key properties emerge from how their paths relate to the real and imaginary axes:

- **Charged leptons** (electron, muon, tau) follow orbits with a nonzero average real projection $\langle m_z \rangle$, giving rest mass, while their interaction with the electromagnetic field shifts $\theta$ and modulates $E$.
- **Neutrinos** are nearly lightlike: their trajectories lie close to the imaginary axis, with very small $m$ but nontrivial phase evolution, which can support flavour oscillations as slow precessions between nearby orbits.
- **Generations** correspond to nested shells in $r$ with similar angular patterns but different characteristic frequencies, reflecting the mass hierarchy without changing the basic complex geometry.

Leptons thus occupy cleaner, less composite regions of the complex plane, making them ideal probes of how $m$ and $E$ trade off along a single worldline.

## Forces as phase symmetries

Forces in the Standard Model act by reshaping or constraining motion on the complex plane rather than by pushing in ordinary space alone. We can sketch them as follows:

- **Electromagnetism** tracks changes in the global phase of charged trajectories. A $U(1)$ gauge transformation is a shift $\theta \mapsto \theta + \alpha$, leaving $r$ fixed but altering interference patterns and detection rates.
- **Weak interactions** mix components of $z$ associated with different leptonic and quark flavours. Geometrically this can be pictured as rotations between nearby orbits in a multi-dimensional complex space, with massive gauge bosons mediating large, localized phase jumps.
- **Strong interactions** constrain colour phases so that only colour-neutral combinations yield closed, low-action paths. Gluon exchange continually rewires how individual quark trajectories share a joint complex-phase structure inside hadrons.

All three gauge forces can be summarised as rules about which deformations of the complex trajectory $z(t)$ leave physical rates invariant and which cost action, echoing the role of symmetries and gauge fields in the usual Standard Model.

## A unified placement

In summary, the complex plane provides a common stage:

- **Quarks** occupy structured, colour-charged orbits whose composites form closed, observable paths.
- **Leptons** trace cleaner, single-particle trajectories distinguished mainly by radius and frequency.

- **Forces** appear as symmetries and constraints on allowed deformations of these complex paths.

This speculative mapping does not replace the field-theoretic Standard Model,[7] but it offers a geometric intuition: all fundamental matter and forces inhabit different patterns of motion and symmetry on an underlying complex $m$–$E$ plane.

# Chapter 7

# Mapping Reality

## 7.1 Reality as projection

The projection postulate—observable reality is $\Re(z) = r\cos\theta$ (Section 2.2.2 of Chapter 2)—has one consequence whose full implications this chapter develops: the projection is **many-to-one**. An infinite number of complex points

$$z_n = a + ib_n, \quad n \in \mathbb{Z} \text{ or } \mathbb{R},$$

all project to the same real value $a$. Each distinct imaginary component $b_n$ represents a different hidden state, a different branch of possibility, yet all manifest identically in observable reality.

This degeneracy is profound: what appears as a single measurement outcome in our three-dimensional reality corresponds to an entire vertical line in the complex plane. The vast multiplicity of states "behind" each observation hints at the richness of the underlying structure.

## 7.2 Precision, dimensionality, and quantization

Conventional physics treats space and time as continuous manifolds with fixed dimensionality (3+1). The EMTS framework suggests a more subtle picture: **dimensionality is conveyed by precision**.

Consider a spatial coordinate $x$. At low precision (coarse-grained measurement), $x$ appears one-dimensional. As we increase precision, we resolve finer structure:

- At scale $\Delta x_1$, position is a single real number
- At scale $\Delta x_2 \ll \Delta x_1$, we resolve additional degrees of freedom: $x = x_{\text{coarse}} + \delta x$
- At Planck scale $\Delta x_P \sim 10^{-35}$ m, quantum geometry emerges, revealing discrete structure

The apparent dimensionality $D_{\text{eff}}$ grows with precision $\epsilon$:

$$D_{\text{eff}}(\epsilon) \sim D_0 + \alpha \log\left(\frac{L_{\max}}{\epsilon}\right),$$

where $D_0$ is the macroscopic dimension, $L_{\max}$ is the largest accessible scale, and $\alpha$ encodes how complexity unfolds at finer scales.

Similarly for time: what appears as a single temporal coordinate $t$ at macroscopic precision becomes a rich structure at finer scales, potentially revealing branching, quantization, or phase-dependent flow rates (as encoded in $\mathcal{N}(x, \rho)$ from the unified framework).

## 7.3 Quantization and the multiverse

The projection degeneracy, combined with precision-dependent dimensionality, naturally leads to a **quantized multiverse structure**.

At each "point" in observable reality $a$, there exists a discrete (quantized) or continuous tower of states parameterized by the imaginary axis:

$$\{z_n = a + ib_n\}_n.$$

The quantization arises from the periodic structure in $\theta$. Physical states must satisfy the single-valuedness condition (cf. “Quantization from closed-orbit conditions” in Chapter 8)

$$\Psi(r, \theta + 2\pi) = \Psi(r, \theta),$$

leading to quantized phase modes:

$$\Psi_n(r, \theta) = R_n(r)\, e^{in\theta}, \quad n \in \mathbb{Z}.$$

Each integer $n$ labels a different "branch" or "universe" characterized by:

- Winding number $n$ around the origin in the complex plane
- Distinct energy spectrum from the Hamiltonian $\hat{H}_\theta = -\frac{\hbar^2}{2I_\theta}\partial_\theta^2 + U_{\text{quad}}(\theta)$
- Different coupling strengths to gauge forces via sector projectors $P_s(\theta)$

### 7.3.1 Many-worlds from many-phases

When a measurement occurs, the projection $z \to \text{Re}(z)$ collapses an infinite-dimensional phase space to a single real outcome. But the framework suggests that **all branches persist in the imaginary direction**. What appears as "wavefunction collapse" in conventional quantum mechanics is simply:

1. Projection: $z = a + ib \to a$ (observable outcome)
2. Persistence: The full state $z = a + ib$ continues to evolve
3. Branching: Different values of $b$ (or equivalently $\theta$) represent parallel realities, all projecting to the same $a$ at the moment of measurement

The multiverse is not a set of disconnected universes, but rather a **continuum of phase-shifted realities**, all coexisting along the imaginary axis, distinguishable only by their internal phase structure $\theta$, which determines:

- Which force quadrant dominates
- The rate of time flow via $\mathcal{N}(x, \rho, \theta)$
- Coupling to different gauge sectors
- Mass-energy partitioning via $\cos\theta$ and $\sin\theta$

### 7.3.2 Cross-branch interference

Although branches with different $\theta$ values project to the same real outcome, they can interfere quantum mechanically. The overlap integral

$$\mathcal{I}_{nm} = \int_0^{2\pi} d\theta \, \Psi_n^*(\theta) \, \hat{O} \, \Psi_m(\theta)$$

describes interference between branches $n$ and $m$ under observable $\hat{O}$. When $\mathcal{I}_{nm} \neq 0$, the branches are not fully independent—they constitute an entangled multiverse.

This framework recovers:

- **Decoherence:** Branches with $\Delta\theta \gg 1$ rapidly dephase, making $\mathcal{I}_{nm} \to 0$
- **Quantum superposition:** States with nearby $\theta$ values maintain coherence
- **Many-worlds interpretation:** Each $\theta$-sector evolves independently when decoherence is complete

## 7.4 Implications for observers

An observer embedded in reality sees only the projection $\mathrm{Re}(z)$. The observer's consciousness, measurement apparatus, and memory all exist in this projected space. Yet the full state $z = a+ib$ evolves according to the complex dynamics.

This creates an epistemic horizon: we can infer the existence of the imaginary component through:

1. **Quantum interference:** The imaginary part influences the evolution of the real part
2. **Entanglement:** Correlations between spatially separated real projections reveal hidden phase structure
3. **Gravitational effects:** The magnitude $r = \sqrt{a^2 + b^2}$ affects spacetime curvature, even though we only observe $a$
4. **Statistical ensembles:** Repeated measurements probe the distribution over $b$, revealing the underlying complex structure

## 7.5 Reconciling continuity and discreteness

The framework unifies apparently contradictory aspects of quantum mechanics and general relativity:

| **Aspect** | **Continuous** | **Discrete** |
|---|---|---|
| Space | Manifold $\mathcal{M}$ | Precision-dependent $D_{\text{eff}}(\epsilon)$ |
| Time | Parameter $t$ | Clock rate $\mathcal{N}(x, \rho)$, phase $\theta$ |
| Phase | Circle $S^1$ | Quantized modes $e^{in\theta}$ |
| Energy | Spectrum of $\hat{H}$ | Eigenvalues $E_n$ |
| Multiverse | Continuum of $\theta$ | Branches labeled by $n \in \mathbb{Z}$ |

At macroscopic scales and low precision, continuity dominates. At microscopic scales and high precision, discreteness emerges. The transition is smooth, governed by the characteristic scales $\hbar$, $c$, and the phase inertia $I_\theta$.

## 7.6 The projection principle

We formalize the central insight:

> *Physical reality is the real projection of a complex state space. Observable phenomena correspond to Re($z$), while the imaginary component Im($z$) encodes hidden degrees of freedom—phase structure, interaction potentials, and alternate branches. Measurement selects a real outcome from an infinite multiplicity of complex pre-images, each representing a distinct universe in the quantized multiverse.*

This projection principle explains:

- Why quantum mechanics is probabilistic (many $z$ map to one $a$)
- Why entanglement is nonlocal (correlations exist in the imaginary direction)
- Why spacetime is dynamical (geometry responds to $|z|$, not just Re($z$))
- Why observers cannot access "other universes" directly (they live in the projection)
- Why precision matters (finer measurements probe finer structure in the complex plane)

Particles are points tracing oscillatory motion; forces emerge as structured relations across quadrants; spacetime geometry echoes these mathematical ties. But beneath it all lies a richer reality: a complex-valued ocean, of which we perceive only the surface.

# Chapter 8

# Quantum Properties on the Complex Plane

Quantum behaviour can be reframed in the EMTS picture established in Chapter 2. Recall that physical states are represented as $z = m + iE = re^{i\theta}$ with $\theta = \omega t$. Projection to the real axis ($r\cos\theta$) encodes what is classically observed, while the full complex motion remains hidden but dynamically essential.

## 8.1 Wave–particle duality as rotating projection

Take a single point $z(t) = re^{i\omega t}$. The real projection

$$m_z(t) = \Re z(t) = r\cos\theta(t)$$

oscillates, while discrete detection events correspond to sampling $m_z$ at particular $\theta$ and locations in $r$. The "wave" is the smooth, complex rotation; the "particle" is the localized real-axis readout.

When several paths $z_k(t)$ are allowed, they add in the complex plane before projection:

$$z_{\text{tot}}(t) = \sum_k z_k(t).$$

Interference patterns arise because $\Re z_{\text{tot}}$ depends on relative angles $\theta_k$, not just moduli $r_k$, mirroring standard complex-amplitude interference described in Chapter 6.

## 8.2 Superposition as geometric addition

A superposed state of two alternatives $A$ and $B$ becomes a vector sum

$$z = \alpha z_A + \beta z_B,$$

with $\alpha, \beta \in \mathbb{C}$ encoding weights and phases. Only after projection does one obtain an outcome associated with $z_A$ or $z_B$, analogous to

$$|\psi\rangle = \cos\theta\,|m\rangle + i\sin\theta\,|E\rangle$$

in Chapter 4. The angle between $z_A$ and $z_B$ in the plane governs constructive or destructive interference in $\Re z$, giving a geometric visualization of the Born rule.

## 8.3 Uncertainty as phase–projection complementarity

If reality is read off as the real projection $m_z = r\cos\theta$, then sharp knowledge of $m_z$ constrains $\theta$ to narrow windows where $m_z$ takes that value. Conversely, if $\theta$ is highly delocalized over $[0, 2\pi)$, many different $m_z$ values are sampled.

Formally, treat $\theta$ as an angle on a circle and its conjugate as an integer winding number $n$ (counting how many $2\pi$ cycles the phase accumulates). Angle–number pairs satisfy an uncertainty relation of the form

$$\Delta n\,\Delta\theta \gtrsim \tfrac{1}{2},$$

which mirrors $\Delta E\,\Delta t$ once $E$ is tied to angular frequency via $E = \hbar\omega$. In EMTS, the spread in $\theta$ (time-like phase) and the spread in $m_z$ (measured mass-like projection) are thus inherently linked, explaining why precise localization in one degrades certainty in the other.

## 8.4 Quantization from closed-orbit conditions

Quantization appears naturally if allowed states correspond to closed or resonant trajectories on the complex circle. Requiring that after an evolution period $T$ the point returns to itself,

$$\theta(T) - \theta(0) = 2\pi n, \qquad n \in \mathbb{Z},$$

imposes discrete conditions on $\omega$ and hence on $E = \hbar\omega$. More generally, demanding single-valuedness of $\Psi(r, \theta)$ on $S^1_\theta$—as in the phase space discussed in Chapter 15—forces integer winding numbers and a tower of allowed modes. The complex circle then acts as a geometric origin for energy levels and other quantized spectra.

## 8.5 Entanglement as correlated complex geometry

For two subsystems $A, B$ with points $z_A = r_A e^{i\theta_A}$ and $z_B = r_B e^{i\theta_B}$, an entangled state can be represented by a joint amplitude $\Psi(z_A, z_B)$ on the product of two complex planes, as developed in Chapter 9. A simple form,

$$\Psi(z_A, z_B) \propto e^{im(\theta_A - \theta_B)},$$

locks their phase difference while leaving the common angle free. Measurements project each point separately to the real axis, but correlations in outcomes reflect the underlying constraint on $(\theta_A, \theta_B)$ and hence on $(m_{z_A}, m_{z_B})$.

In this view, entanglement is not mysterious action at a distance but a single geometric object on $(z_A, z_B)$ space whose projections on separate real axes remain correlated even when $r_A$ and $r_B$ are widely separated.

## 8.6 Summary

Wave–particle duality, superposition, uncertainty, quantization, and entanglement all become features of how complex points move, add, and close on the EMTS plane, and how partial projections slice this richer geometry into the classical realities we observe.

# Part III

# Implementation

# Chapter 9

# Entanglement on the Complex Plane

## 9.1 Framing EMTS variables for entanglement

Recall from Chapter 2 that EMTS represents physical events as points on the complex plane $z = m + iE = re^{i\theta}$, with $r$ encoding space and $\theta$ encoding time. Two-system entanglement can be modeled on pairs $(z_A, z_B)$ by building joint states and correlators that respect EMTS' polar structure. In this view, time has two aspects: a monotone history variable (global $\theta$-translation) and a periodic phase (modulo $2\pi$), which naturally invites resonance phenomena and Floquet-like behavior in $\theta$ space.

## 9.2 A minimal mathematical insertion

### 9.2.1 State, reduction, and $\theta$-symmetry

- **Global state:** Let $|\Psi\rangle$ live on a Hilbert space over EMTS points; for two subsystems $A, B$ at $z_A = r_A e^{i\theta_A}$, $z_B = r_B e^{i\theta_B}$, write the joint amplitude $\Psi(z_A, z_B)$.[4]
- **Entanglement test:** Compute $\rho_A = \mathrm{Tr}_B\, |\Psi\rangle\langle\Psi|$ and a measure $S_A = -\mathrm{Tr}(\rho_A \log \rho_A)$ (or a negativity). Entanglement is present iff $\rho_A$ is mixed.
- **$\theta$-translation invariance:** If dynamics and initial conditions are invariant under simultaneous shifts $\theta_A \to \theta_A + \alpha$, $\theta_B \to \theta_B + \alpha$, then any entanglement measure depends only on the phase difference $\Delta\theta = \theta_A - \theta_B$ and the radii $(r_A, r_B)$, not on absolute $\theta$ (stationarity):

$$\partial_\Theta S_A = 0, \quad \Theta = \tfrac{1}{2}(\theta_A + \theta_B).$$

### 9.2.2 Interaction kernels on the complex plane

- **Phase-sensitive coupling:**

$$H_{\text{int}} = \lambda\, f(r_A, r_B)\, \cos(\Delta\theta - \phi_0)\, \hat{O}_A \otimes \hat{O}_B,$$

  which entangles $A$ and $B$ when $f \neq 0$. The $\cos(\Delta\theta)$ factor makes phase relations explicit; $\phi_0$ sets a preferred phase alignment.

- **Holomorphic form (optional):**

$$H_{\text{int}} = \lambda\, g(z_A, z_B)\, \hat{O}_A \otimes \hat{O}_B + \text{h.c.},$$

  with $g$ holomorphic to ensure Cauchy–Riemann compatibility in EMTS. This yields entanglement protected along contours of constant argument or modulus depending on $g$.

## 9.3 Resonance as phase-locking in $\theta$-time

- **Phase-locked entanglement:** If time has a periodic component, entanglement can strobe at resonant phase differences. With a drive of frequency $\omega$ on $\theta$, stroboscopic evolution produces
$$U_F = e^{-iH_{\text{eff}}T}, \quad T = \tfrac{2\pi}{\omega},$$
and entanglement peaks when $\Delta\theta$ satisfies locking conditions (e.g., $\Delta\theta \approx \phi_0 \bmod 2\pi$).
- **Growth vs. invariance:** In generic (chaotic) dynamics, entanglement exhibits universal growth and saturation patterns (e.g., area-law to volume-law crossover with velocity $v_E$). "Entanglement is independent of time" can be realized when the initial state and generator are $\theta$-stationary so only $\Delta\theta$ matters, or when a resonance creates steady phase-locking so the entanglement measure becomes $\theta$-periodic and effectively constant under coarse graining.

## 9.4 Time independence and projection on the real axis

- **Projection choice matters:** If "projected on the real axis" means evaluating observables at fixed $\theta$ (equal-time slice), entanglement reduces to a function of radii and their separation along $r$, i.e., $S_A = S_A(r_A, r_B, \Delta\theta)$ with $\Delta\theta = 0$. With $\theta$-translation invariance, this yields entanglement profiles depending only on spatial relations in $r$.
- **Integrating out $\theta$:** Alternatively, integrating phases (or averaging over $\Theta$) leaves phase-invariant correlators:
$$\overline{C}(r_A, r_B) = \frac{1}{2\pi}\int_0^{2\pi} d\Theta\; C(r_A e^{i(\Theta+\Delta\theta/2)},\, r_B e^{i(\Theta-\Delta\theta/2)}).$$

## 9.5 Testable consequences and a concrete ansatz

### 9.5.1 A simple EMTS entangled pair

$$\Psi(z_A, z_B) = \frac{1}{\sqrt{2}}\Big[\phi_0(r_A)\phi_1(r_B)\, e^{im(\theta_A-\theta_B)} + \phi_1(r_A)\phi_0(r_B)\, e^{-im(\theta_A-\theta_B)}\Big].$$

- **Label:** $m$ is a winding in $\Delta\theta$; $\phi_{0,1}$ control localization in $r$.
- **Property:** Entanglement is maximal and independent of $\Theta$; tuning $m$ sets resonance channels in $\Delta\theta$.

### 9.5.2 Dynamics with resonance

Use $H_{\text{int}}(t) = \lambda(t)\, f(r_A, r_B)\cos(\Delta\theta - \phi_0)\, \hat{O}_A \otimes \hat{O}_B$ with $\lambda(t+T) = \lambda(t)$. Predict:

- **Locking:** Stable entanglement plateaus at $\Delta\theta \approx \phi_0$.
- **Velocity bounds:** Expect entanglement growth bounded by an effective $v_E$ and shaped by a "line tension," analogous to results in Floquet and chaotic circuits.
- **Equal-$\theta$ slices:** On $\Delta\theta = 0$, entanglement reduces to spatial profiles along $r$.

## 9.6 Bridge to EMTS geometry

### 9.6.1 Core translation

Any normalized two-level state can be written

$$|\psi\rangle = \cos\theta\,|m\rangle + i\,\sin\theta\,|E\rangle,$$

so the geometric angle $\theta$ from $z = re^{i\theta}$ becomes the parameter in the quantum superposition. Measurements use projectors like $P_m = |m\rangle\langle m|$ giving $P(m) = \cos^2\theta$. A simple Hamiltonian $H = (\hbar\omega/2)\,\sigma_y$ rotates probability between $|m\rangle$ and $|E\rangle$ at angular frequency $\omega$.[4]

### 9.6.2 Link to the geometry

The real-axis projection in the complex picture becomes applying $P_m$ in Hilbert space; "collapse" corresponds to projecting $z$ to $\mathrm{Re}(z)$ and normalizing. The radial coordinate $r$ controls overall scale but is factored out in quantum normalization.

# Chapter 10

# Feynman Diagrams on the Complex Plane

Let's reinterpret Feynman diagrams within the EMTS framework (Chapter 2). Instead of drawing them in the usual spacetime coordinates, plot each particle's state $z = m + iE = re^{i\theta}$ in the mass–energy plane. Each line in a diagram becomes a curve

$$\gamma(\lambda) : [0, 1] \to \mathbb{C}, \qquad \gamma(\lambda) = r(\lambda)e^{i\theta(\lambda)},$$

with $\lambda$ a path parameter. External legs are *open* curves, anchored to asymptotic "in" and "out" states, while internal lines and loops can form *closed* or self-intersecting curves that encode virtual processes.

## 10.1 Particles as trajectories in the plane

- **External legs:** Each external particle is an open curve in the complex plane from an initial $z_i$ to a final $z_f$, representing how its mass–energy configuration evolves between preparation and detection.
- **Massive vs. massless:** Massless particles (photons, gluons) follow paths hugging the imaginary axis; massive particles trace tilted paths with significant real component.
- **Neutrinos:** Almost vertical lines near the imaginary axis, with tiny real offset.
- **Quarks:** Confined loops in the strong-force quadrant, never escaping to free-particle regions.

In this picture, a conventional Feynman diagram is not just a graph of lines and vertices but a collection of curves $\{\gamma_i\}$ drawn on the same complex plane, meeting at junctions that enforce complex conservation laws.

## 10.2 Vertices as junctions of complex vectors

A vertex is a point where several $z$-vectors meet, and complex-vector conservation applies:

$$\sum_{\text{in}} z = \sum_{\text{out}} z.$$

The quadrant in which the vertex sits indicates the mediating force (see Chapter 5: $Q_{\text{I}}$ for EM, $Q_{\text{II}}$ for weak, $Q_{\text{III}}$ for strong, $Q_{\text{IV}}$ for gravitational).

## 10.3 Propagators as arcs or spirals

- **Massive propagator:** Spiral with both radial and angular change (space and time evolution).
- **Massless propagator:** Pure angular advance at fixed radius (lightlike).
- **Virtual particles:** Paths that wander into "unphysical" quadrants or cross branch cuts; their projection on the real axis may be zero or negative.

Each propagator thus corresponds to a family of admissible curves between two points $z_a$ and $z_b$. In a path-integral spirit, the physical amplitude weights these curves by a phase factor depending on the "action" along the path in the complex plane.[7]

## 10.4 Curves and amplitudes

For a given scattering process, standard quantum field theory assigns an amplitude by summing over all compatible Feynman diagrams. In the complex-plane view, this becomes a sum over classes of curves:

$$\mathcal{A}_{\text{process}} \sim \sum_{\text{diagrams}} \sum_{\{\gamma_i\}} e^{iS[\{\gamma_i\}]},$$

where the action functional $S[\{\gamma_i\}]$ depends on how the curves wind, which quadrants they traverse, and how they meet at vertices. Open curves carry the quantum numbers of external particles, while closed curves (loops) encode vacuum fluctuations and radiative corrections.

In this hypothesis, momentum conservation and on/off-shell conditions translate into geometric constraints on allowed curve shapes and endpoints in the $m$–$E$ plane. Different diagram topologies then correspond to different homotopy classes of curve-collections, offering a topological handle on selection rules and interference.

## 10.5 Loops and quantum corrections

Loop diagrams in QFT become closed loops in the complex plane.[7] The winding number of the loop can correspond to a conserved quantum number (charge, baryon number). Divergences may appear as loops that shrink toward the origin $z = 0$, requiring renormalization as a deformation away from the singularity.

## 10.6 Example: Electron–neutrino scattering

- **Initial state:** Electron $z_e$ in $Q_{\text{I}}$ ($0 < \theta_e < \pi/2$, positive mass and energy), neutrino $z_\nu$ near imaginary axis.
- **Vertex:** Weak-force quadrant (Q2), where a W boson is exchanged.
- **Propagator:** W boson path arcs from electron's $z$ to neutrino's $z$, crossing the imaginary axis.
- **Final state:** New $z$ positions for outgoing electron and neutrino, conserving the complex sum.

## 10.7 Why this is interesting

- **Unified conservation:** Mass and energy conservation become one complex equation at each vertex.
- **Virtuality geometry:** Off-shell particles are "off-axis."
- **Topological insight:** Winding numbers and quadrant crossings give visual handles on selection rules and forbidden processes.

# Chapter 11

# Periodic Table Analogy

Could the EMTS framework play a role similar to the periodic table in hinting at missing pieces? The periodic table worked because its arrangement was a geometry of relationships; gaps were structural necessities. The complex-plane paths and diagram reinterpretations have similar potential if the geometry demands certain configurations.

## 11.1 How unknowns could emerge

### 11.1.1 Topology demands missing states

If winding numbers, quadrant crossings, or density-dependent phase rules are strict, certain interaction vertices only balance if a missing $z$-vector exists. That vector could correspond to an undiscovered particle, a new interaction, or a composite state.

### 11.1.2 Symmetry completion

If the diagram set respects a symmetry (rotational in $\theta$, reflection across axes), incomplete multiplets stand out—like polygons in the complex plane with a missing vertex.

### 11.1.3 Forbidden gaps as clues

Absence of a path can be telling: if quadrant transitions are allowed by geometry but never observed, that could indicate a hidden law or a very heavy/weakly coupled particle.

### 11.1.4 Density–phase resonance

With $\omega(\rho)$ tied to density, there may be resonant densities where paths close neatly in $\theta$ after an integer number of $2\pi$ cycles. Gaps in a resonance sequence suggest missing states.

## 11.2 What this could predict

New neutrino-like states, exotic hadrons, force carriers (dark photon), or leptoquarks could fill geometric gaps implied by closure rules and symmetries.

## 11.3 How to search

Catalogue known particles in $(m, E, r, \theta)$, map interaction paths, look for incomplete geometric patterns, and infer the missing $z$: its quadrant, radius, and phase give mass, energy, and coupling hints.

# Chapter 12

# Chemical Activation Analogue

This section borrows the logic of chemical activation diagrams and transplants it into the mass–energy–phase plane.

## 12.1 Analogy

In chemistry, an activation diagram plots potential energy vs. reaction coordinate. Here, the "reaction coordinate" is a path in $(r, \theta)$: initial $z_i = r_i e^{i\theta_i}$, final $z_f = r_f e^{i\theta_f}$, and a barrier as a dynamically disfavoured region.

## 12.2 Activation mass–energy

The activation energy becomes an activation mass–energy: the extra $|z|$ or angular displacement needed to connect two states.

## 12.3 Manipulating mass/energy

- **Catalysis analogue:** Introduce an intermediate path bending through a quadrant with a lower barrier; mediators or fields change the allowed trajectory so the peak $|z|$ is smaller.
- **Phase-assisted transitions:** Because $\theta$ is cyclic, one can wrap around instead of going straight over, akin to tunnelling.
- **Density-tuned activation:** If $\omega(\rho, r)$ changes effective heights, altering local density can lower the barrier via phase-resonance.

## 12.4 Diagrammatic representation

Plot total $|z| = r$ vs. path length along $(r, \theta)$; different complex-plane paths yield different activation curves.

## 12.5 Formalization

Define an activation functional for a path $\gamma$:

$$\mathcal{A}[\gamma] = \max_{s \in \gamma} \big[ r(s) - \min(r_i, r_f) \big],$$

and search for paths minimizing $\mathcal{A}$ subject to complex-plane conservation laws. Catalysts, fields, or density changes are deformations of $U(r,\theta)$ that reduce $\mathcal{A}$.

# Chapter 13

# Celestial Mechanics

## 13.1 Motivation: the dual nature of the electron

The electron is simultaneously a particle and a wave. As a particle it carries a well-defined mass $m_e$ and charge $-e$; as a wave it is described by a complex-valued wavefunction $\psi(\mathbf{x}, t) = |\psi|\, e^{i\phi}$ that obeys the Schrödinger (or Dirac) equation. When many-electron wavefunctions overlap, the phases $\phi_k$ can align or oppose, producing entirely new macroscopic states that bear little resemblance to the bare electron.

Within the EMTS framework the electron sits at

$$z_e = m_e + iE_e = r_e\, e^{i\theta_e},$$

where $r_e = \sqrt{m_e^2 + E_e^2}$ is the total mass-energy magnitude and $\theta_e = \arctan(E_e/m_e)$ records the partition between rest mass and kinetic/potential energy. For a free electron at rest $\theta_e \approx 0$ (real axis), while a high-energy electron is rotated toward the imaginary axis.

A *collective* state of $N$ electrons is then described by the vector sum

$$Z_{\text{coll}} = \sum_{k=1}^{N} z_k = \sum_{k=1}^{N} r_k\, e^{i\theta_k}.$$

The character of this sum — constructive or destructive — determines whether the system behaves as an **Angel** or a **Demon** in the taxonomy developed below. The Demon concept draws its name and its physical content from the charge-neutral, acoustic collective mode first predicted by Pines in 1956,[8] whose analysis showed that destructive interference among electron contributions can produce a quasi-particle that hides from conventional electromagnetic observation.

## 13.2 Constructive interference: Angels

### 13.2.1 Definition

Consider $N$ electrons whose EMTS phases are *aligned*:

$$\theta_k \approx \bar{\theta} \quad \forall\, k.$$

The collective vector is then approximately

$$Z_{\text{Angel}} \approx \left( \sum_{k=1}^{N} r_k \right) e^{i\bar{\theta}},$$

which is a single EMTS point with modulus $\sim Nr_e$ and essentially the same argument as the individual electrons. The real (mass-like) and imaginary (energy-like) components both scale up together.

### 13.2.2 Physical content

Phase alignment means that maxima of the individual wavefunctions coincide. Some familiar realizations:

- **Cooper pairs and superconductivity.** Below $T_c$, electrons near the Fermi level pair into Cooper pairs with equal and opposite momenta and opposite spins; their pair wavefunction is a single coherent superposition. In EMTS, the pair amplitude has its phases locked so that $Z_{\text{pair}}$ sits solidly on the real axis (dominant mass, minimal energy dispersion), explaining the gap and lossless transport.[1]
- **Coherent many-body ground states.** In a crystal, Bloch electrons form bands; near a filled lower band the coherent sum of occupied states gives a stable, low-energy configuration — the background "sea" of condensed matter.
- **Stimulated emission.** In a laser medium, photon-driven transitions reinforce phase alignment of atomic dipoles; the emitted photons are the EM analogue of the Angel state.

### 13.2.3 EMTS geometry

In the complex plane, an Angel state corresponds to a tight *cluster* of $N$ points near a single $z_e$, their vector sum pointing radially outward with length $\sim Nr_e$. The projection $\Re(Z_{\text{Angel}}) = Nr_e \cos\bar{\theta}$ is large: Angels are *observable* in the real (mass/matter) sector.

## 13.3 Destructive interference: Demons

### 13.3.1 Definition

Now suppose the phases of the participating electrons are *anti-aligned*:

$$\theta_k = \bar{\theta} + \delta_k, \quad \sum_{k=1}^{N} e^{i\delta_k} \approx 0.$$

In the simplest two-electron toy model with $\theta_1 = \theta$ and $\theta_2 = \theta + \pi$:

$$Z_{\text{Demon}} = r_1 e^{i\theta} + r_2 e^{i(\theta+\pi)} = (r_1 - r_2)\, e^{i\theta}.$$

When $r_1 = r_2$ the individual mass-energy contributions *cancel exactly*: $Z_{\text{Demon}} = 0$. Even when cancellation is only partial, the dominant real-axis component is suppressed, and what survives is primarily imaginary — *energy without mass.*

### 13.3.2 Electrons as plasmons

The most experimentally dramatic Demon is the *plasmon* — the collective charge-density oscillation of the electron gas.[1] A classical derivation illustrates the Demon mechanism:

1. Each conduction electron in a metal has individual EMTS vector $z_k = m_e + iE_k$.

2. A charge displacement excites a density wave $n(\mathbf{x}, t) = n_0 + \delta n \cos(\mathbf{q} \cdot \mathbf{x} - \omega t)$.

3. The restoring Coulomb forces couple all electrons so that individual particle identities dissolve into a collective mode at the plasma frequency

$$\omega_p = \sqrt{\frac{n_0 e^2}{\epsilon_0 m_e}}.$$

4. This new quasi-particle — the *plasmon* — has an effective mass determined by $\omega_p$ and a dispersion $\omega(\mathbf{q})$ very different from the bare electron.

In EMTS, the plasmon is described not by any single $z_k$ but by the *residual* of the collective sum after destructive cancellation. Its EMTS vector sits near the imaginary axis (large $\theta$, small real component), reflecting the fact that the plasmon has very little "matter-like" character — it is primarily an *energy excitation* propagating through the electron sea.

### 13.3.3 The Demon analogy

The metaphor of the *Demon* is apt:

- Like a demon, the plasmon exploits the absence of order (destructive phase cancellation) to manifest as something qualitatively different from the individual electrons.
- It "hides" behind the anti-phase interference — invisible to direct mass measurement, yet capable of transporting energy at $\omega_p$ and mediating optical phenomena at UV frequencies.
- Demons are *unnatural* in the sense that they require a specific cancellation to persist; they depend on the maintenance of phase opposition across the participating electrons.

### 13.3.4 EMTS geometry

In the complex plane, the individual electron points spread symmetrically around the origin so that their vector sum $Z_{\text{Demon}}$ is close to (or exactly at) zero. The plasmon is then the *phase-space excitation* of this near-cancellation — a small residual that rotates rapidly near the imaginary axis, with $|\Re(Z)| \ll |\Im(Z)|$.

## 13.4 An EMTS taxonomy of collective electron modes

The constructive/destructive axis is not binary. We can organize all collective electron states on a spectrum according to the degree of phase coherence in the EMTS sum. Four named classes arise naturally, analogous to a celestial hierarchy:

| **Name** | **Phase relation** | $\lvert Z_{\mathbf{coll}}\rvert / N r_e$ | **Physical archetype** |
|---|---|---|---|
| Archangel | Extreme constructive, $\delta_k \to 0$ | $\to 1$ | BEC, superfluid, lasing mode |
| Angel | Constructive, partial alignment | 0.5 to 1 | Cooper pairs, band ground state |
| Mixed | Transitional, partial coherence | 0.1 to 0.5 | Normal metal, thermal electron gas |
| Demon | Destructive, partial cancellation | $\lesssim 0.1$ | Plasmons, acoustic modes |
| Devil | Extreme destructive, near-total cancel | $\to 0$ | Acoustic plasmon, demon quasi-particle |

### 13.4.1 Angels: the natural order

Constructive interference is the *ground-state tendency*: a system of electrons minimizes its energy by occupying coherently the lowest available modes, with wavefunctions adding positively. Angels represent equilibrium. Left to evolve without perturbation, an electron ensemble relaxes toward an Angelic configuration because such states minimize free energy.

### 13.4.2 Archangels: extreme coherence

When phase alignment is *forced* across a macroscopic number of particles — as in a Bose-Einstein condensate (BEC), a superfluid, or an optical laser — the collective EMTS vector points almost perfectly along a single direction in the complex plane, with $|Z| \approx N r_e$. This is the Archangel limit:

$$Z_{\text{Arch}} = N r_e \, e^{i\bar{\theta}}, \qquad \text{all } \theta_k \equiv \bar{\theta}.$$

Archangels are extraordinary: they require macroscopic phase locking, typically enforced by a symmetry-breaking mechanism (BCS gap equation, Gross-Pitaevskii condensation, stimulated emission). Their EMTS projection on the real axis is the largest possible, making them the *most observable* collective electron states.

### 13.4.3 Demons: the plasmon family

Standard plasmons (bulk, surface, acoustic) form the core of the Demon class. Their salient EMTS property is:

- Small $|\Re(Z_{\text{coll}})|$ — minimal "matter" character.
- Large $|\Im(Z_{\text{coll}})|$ / fast $\theta$ rotation — dominant energy character.
- Finite lifetime: phase opposition is maintained only for the coherence time $\tau_p$; scattering and damping (Landau damping) restore the Angel ground state.

The surface plasmon polariton (SPP) is a Demon that lives at the interface between a conductor and a dielectric, coupling to photons — a mixed photonic/electronic Demon with EMTS vector straddling both electromagnetic and material quadrants.

### 13.4.4 Devils: extreme destructive states

The Devil limit is total cancellation $Z \to 0$. This requires fine-tuning or protective symmetry. Known physical candidates:

- **Acoustic plasmon & the "electronic Demon."** In a multi-band metallic system where two bands with nearly equal but opposite effective-mass contributions coexist, destructive cancellation of the conventional Drude weight can yield a mode that propagates *without electromagnetic restoring force* — a massless, charge-neutral collective oscillation. David Pines predicted exactly this mode in 1956[8]: he showed that in a two-component electron fluid the conventional plasmon (a Devil in the EMTS taxonomy) acquires an acoustic branch that carries no net charge and couples minimally to photons — a "demon" in the literal sense of an entity that hides from direct observation. Nearly seven decades later the mode was observed experimentally in terbium-based intermetallic compounds,[5] confirming Pines' original prediction and its charge-neutral, acoustic character at $q = 0$.

- **Topological surface states.** In topological insulators, bulk states cancel (Devil bulk) while surface states remain, protected by topology.
- **Dark states in quantum optics.** A coherent superposition of atomic dipoles designed to have zero net coupling to the radiation field is a "dark" or Devil state — it stores coherence invisibly.

In EMTS, a Devil has $Z_{\text{coll}} \approx 0$: the collective state is invisible on the real axis and carries negligible imaginary component too. Energy is locked into phase-space correlations rather than carried by the field amplitude.

## 13.5 Dynamics: transitions between classes

The four classes are not static. An electron system can transit between them driven by temperature, field, or interaction:

$$\text{Archangel} \xrightarrow{\text{heat / disorder}} \text{Angel} \xrightarrow{\text{drive / pump}} \text{Demon} \xrightarrow{\text{fine-tune}} \text{Devil}.$$

In EMTS language each transition corresponds to a *rotation* of the cluster of $z_k$ points:

- **Heating:** thermal fluctuations spread the $\theta_k$ uniformly, reducing $|Z_{\text{coll}}|$ toward zero (Archangel $\to$ Devil).
- **Driving with a laser:** a pump pulse can align all phases, pushing from Demon to Angel (Demon $\to$ Angel, cf. ultrafast demagnetization and light-induced superconductivity).
- **Band engineering:** designing a material so that two electron bands have exactly opposite Drude weights creates a stable Devil state; the EMTS sum stays near zero even at low temperature.[5]

## 13.6 A Pindaric Flight: Protons, Color, and the Strong Force

*This section is deliberately speculative. It extends the Angels-and-Demons framework beyond its established condensed-matter ground and asks whether the same wave-interference logic governs the strong nuclear force. The reader is invited to treat what follows as a conjecture rather than a derivation.*

### 13.6.1 The proton as a collective state

The proton is not an elementary particle. It is made of three quarks ($uud$), each carrying one of three *color charges* — called Red, Green, and Blue — bound together by the exchange of gluons. What emerges is electrically charged, massive, and confined: no free quark has ever been observed. The question we raise here is: can the same phase-interference mechanism that produces plasmons from electrons produce the *strong force* from quarks?

In EMTS, each quark carries a mass-energy vector $z_q = m_q + iE_q$ as before. But it also carries an *internal color phase* $\phi_c$, which we treat as an additional angular degree of freedom orthogonal to the EMTS time-phase $\theta = \omega t$ and distinct from the single-electron wavefunction phase $\phi$ introduced in Section 13.3. Three angles thus appear in this chapter and the reader should keep them separate: $\phi$ (microscopic wavefunction phase of a single electron), $\theta$ (the EMTS

mass–energy angle, identified with time via $\theta = \omega t$, and used throughout this book), and $\phi_c$ (internal color phase living in the $SU(3)$ color space, introduced only in this section). We write the full quark state schematically as

$$\tilde{z}_q = z_q \cdot e^{i\phi_c},$$

where $\phi_c \in \{0,\, 2\pi/3,\, 4\pi/3\}$ for the Red, Green, and Blue quarks respectively.

### 13.6.2 The color-Devil condition

Consider the three quarks in a proton and form their color-phase sum:

$$Z_{\text{color}} = e^{i\cdot 0} + e^{i\cdot 2\pi/3} + e^{i\cdot 4\pi/3} = 1 + \left(-\tfrac{1}{2} + i\tfrac{\sqrt{3}}{2}\right) + \left(-\tfrac{1}{2} - i\tfrac{\sqrt{3}}{2}\right) = 0.$$

This is the **Devil condition** applied to color space. The three quark color phases are placed exactly 120° apart on the unit circle and cancel completely — a perfect three-way destructive interference. In EMTS terms:

- $|Z_{\text{color}}| = 0$: the proton has no net color charge. It is "color-invisible."
- The individual quarks are not observable ($|z_q| \neq 0$, color charge exposed); only the Devil combination $Z_{\text{color}} = 0$ can propagate freely.

This is *color confinement* restated in the language of the Angel/Demon taxonomy: **Nature requires every free particle to satisfy the color-Devil condition.** What we call "the strong force" is, in this reading, the mechanism that enforces it.[3]

### 13.6.3 Why this is deeper than the electron Demon

In the electron case the Demon (plasmon) arises as a collective excitation *above* an Angel ground state. Destructive interference is an excited, transient phenomenon; the ground state is constructive. For quarks the situation is inverted:

- The color-Devil condition is the *ground state requirement* — particles that do not satisfy it are confined and never free.
- The "color Angel" limit — a state with net color charge — would correspond to a free quark. It has never been observed at low energies, though it is approached in the quark-gluon plasma (QGP) at extreme temperature and density (see below).

The electron Demons are fragile and short-lived; the color Devil is permanent at low energy. The strong force is *so* strong precisely because the Devil condition is enforced with energy cost that grows with separation (confinement), unlike the Coulomb force, which weakens with distance.

### 13.6.4 Gluons as color Demons

In the electron gas, the Demon (plasmon) is a collective excitation of the electron field — a Demon that mediates energy transfer without carrying net charge. The gluon plays an analogous role for the color field, but with a crucial difference:

- A **photon** is charge-neutral — the EM Demon does not carry the charge it mediates.

- A **gluon** carries *color charge* itself (e.g., a red-anti-green gluon). The color Demon is *self-interacting*.

This self-interaction of the color Demon is the origin of *asymptotic freedom* (at short distances, gluon self-coupling weakens) and *confinement* (at long distances, gluon self-coupling creates a flux tube whose energy grows linearly with separation). In EMTS, the self-interacting Demon feeds back into the color-phase sum: every gluon emission re-colors one quark, immediately reshuffling the color phases to maintain $Z_{\text{color}} = 0$.

### 13.6.5 Pions as two-body color Devils and the nuclear force

A pion ($\pi^+ = u\bar{d}$, $\pi^- = \bar{u}d$, $\pi^0 = u\bar{u}/d\bar{d}$) is a quark-antiquark pair. Its color phase sum is simpler:

$$Z^{\pi}_{\text{color}} = e^{i\phi_c} + e^{i(\phi_c+\pi)} = 0,$$

since a quark of color $\phi_c$ and its antiquark of anti-color $\phi_c + \pi$ destructively cancel in a *two-body* color Devil. The pion is much lighter than the proton (mass $\approx 140$ MeV vs. 938 MeV) because it is the pseudo-Goldstone boson of spontaneously broken chiral symmetry: it costs very little energy to create a two-body color Devil, making it the natural *carrier* of the residual nuclear force between protons and neutrons. In EMTS, the pion is a color-Devil mediator: its $Z_{\text{color}} = 0$ lets it travel between hadrons without violating confinement, transferring momentum and binding the nucleus.

### 13.6.6 The quark-gluon plasma: melting the color Devil

At temperatures above $T_c \approx 150$ MeV (achieved in heavy-ion collisions at RHIC and LHC), hadronic matter deconfines into a *quark-gluon plasma* (QGP). In EMTS language:

- Below $T_c$: quarks are locked into color-Devil configurations (hadrons). The color-phase sum is $Z_{\text{color}} = 0$ for every observable state.
- Above $T_c$: thermal fluctuations are energetic enough to break the color-Devil constraint. Color-charged quarks roam freely — the system acquires a nonzero, fluctuating $Z_{\text{color}}$ in each local region. This is the color-Angel (or color-Archangel) limit.

The QGP phase transition is therefore the color analogue of breaking Cooper pairs above $T_c$ in a superconductor: an Archangel (BCS superfluid) melts into a normal electron gas (Angel/Demon) as temperature rises. Here the color-Devil (hadron) melts into a color-Angel (free quark) as temperature rises.

### 13.6.7 A tentative EMTS conjecture

Bringing the thread together: the fundamental forces can be tentatively classified by *which type of EMTS interference condition they enforce*:

| **Force** | **Enforced condition** | **Free-particle rule** |
|---|---|---|
| Electromagnetism | No condition on phase | Charged particles propagate freely |
| Weak force | $SU(2)$ phase alignment (Angel) | Broken at low $E$ by Higgs |
| Strong force | Color-Devil ($Z_{\text{color}} = 0$) | Only color-neutral states are free |
| Gravity | Spacetime curvature (EMTS radial) | All massive objects curve $r$ |

In this reading, the strong force is *the Devil force*: it is the force that imposes the most extreme destructive-interference condition on its constituents, making its bound states ($Z_{\text{color}} = 0$) uniquely stable and its individual constituents (quarks) permanently hidden.

Whether this is merely a suggestive analogy or points toward a deeper unification within the EMTS framework remains an open question — one we leave to future chapters and future physicists.

## 13.7 A Second Pindaric Flight: Neutrinos as Natural Devils

*This section is deliberately speculative. It extends the Angels-and-Demons framework beyond its established condensed-matter ground and argues that the neutrino — the most ghost-like of all known fermions — is not merely analogous to a Demon but belongs squarely in the* ***Devil*** *class: a fundamental particle whose mass-energy vector is permanently confined near the origin by the very structure of its mass generation, satisfying an extreme destructive-interference condition that no composite quasi-particle in condensed matter can match.*

### 13.7.1 The neutrino: a particle that hides

The neutrino is, by almost every measure, the most elusive massive particle in the Standard Model:

- It carries no electric charge and no color charge.
- Its mass is non-zero but extraordinarily small ($m_\nu \lesssim 0.1$ eV, compared to $m_e \approx 511$ keV).
- It couples only to the weak force and gravity — the two weakest interactions at low energy.
- It is produced and detected exclusively in flavor eigenstates ($\nu_e, \nu_\mu, \nu_\tau$) that are *quantum superpositions* of mass eigenstates ($\nu_1, \nu_2, \nu_3$).
- Trillions of solar neutrinos pass through every square centimetre of your body each second without interaction.

The neutrino hides. It is not merely a Demon — it is a **Devil**: a fermion whose "matter-like" (real-axis) EMTS component is suppressed to the point of near-total cancellation, placing it at the extreme end of the celestial hierarchy rather than merely near it.

### 13.7.2 The neutrino in the EMTS complex plane

For a relativistic neutrino of flavor $\alpha$ and momentum $|\mathbf{p}| \gg m_\nu$, the energy is $E \approx |\mathbf{p}|$ and the rest mass is negligible. Its EMTS vector is

$$z_\nu = m_\nu + iE_\nu \approx iE_\nu,$$

which lies almost exactly on the *imaginary axis*: $\theta_\nu = \arctan(E_\nu/m_\nu) \approx \pi/2$. The real-axis residue is

$$\frac{|\Re(z_\nu)|}{|z_\nu|} = \frac{m_\nu}{E_\nu} \sim 10^{-10} \quad \text{(for a typical solar neutrino)}.$$

The taxonomy table places Demons at "small $|Z|$, near imaginary axis" and Devils at "$|Z| \approx 0$, near origin." A ratio of $10^{-10}$ is unambiguously Devil territory. No bulk plasmon, surface plasmon polariton, or acoustic Demon in condensed matter comes anywhere close: all of them

retain a real-axis component of order $10^{-1}$ to $10^{-3}$ at most. The free neutrino is a **fundamental Devil** — the only known elementary particle that lives, by design, at the extreme-destructive end of the EMTS hierarchy.

### 13.7.3 Flavor oscillations as interference between Devils

The deepest weirdness of the neutrino is flavor oscillation: a $\nu_e$ produced in a nuclear reaction is detected, after traveling macroscopic distances, as a $\nu_\mu$ or $\nu_\tau$. The standard description invokes a unitary mixing matrix (the PMNS matrix), but in EMTS language the phenomenon is transparently an *interference* effect.

Each mass eigenstate $\nu_j$ ($j = 1, 2, 3$) has its own EMTS time-evolution phase $e^{-iE_j t}$, and to a good approximation $E_j \approx |\mathbf{p}| + m_j^2/(2|\mathbf{p}|)$. The flavor eigenstate is

$$|\nu_\alpha(t)\rangle = \sum_{j=1}^{3} U_{\alpha j}\, e^{-iE_j t}\, |\nu_j\rangle.$$

The survival and transition probabilities are proportional to

$$P(\nu_\alpha \to \nu_\beta) \propto \left| \sum_j U_{\alpha j}^* U_{\beta j}\, e^{-i\Delta m_{j1}^2 L/2|\mathbf{p}|} \right|^2,$$

where $L$ is the propagation distance. This is exactly the two-slit interference formula — the three mass eigenstates play the role of three slits, and the oscillation length $L_{\text{osc}} = 4\pi|\mathbf{p}|/\Delta m^2$ is the analogue of fringe spacing.

In EMTS, each $|\nu_j\rangle$ is a separate Devil vector $z_j$ near the imaginary axis, rotating at a slightly different frequency $\omega_j = E_j/\hbar$. The *flavor* state is the running sum

$$Z_{\nu_\alpha}(t) = \sum_{j=1}^{3} U_{\alpha j}\, r_j\, e^{i(\phi_j - \omega_j t)},$$

which oscillates between constructive and destructive configurations as the phases drift apart. **Flavor oscillation is a Devil-to-Devil transition**: the collective EMTS vector beats among three near-origin configurations, never acquiring a significant real-axis component, never becoming an Angel. The oscillation length $L_{\text{osc}}$ is large precisely because the three Devil vectors are nearly identical — a small phase difference between near-cancelling amplitudes produces slow beating, just as two nearly-equal Demon amplitudes in a condensed-matter system produce long-wavelength charge-density oscillations.

### 13.7.4 Majorana neutrinos: the self-conjugate Devil

Whether the neutrino is a Dirac or Majorana fermion remains experimentally open. A Majorana neutrino is its own antiparticle: $\nu = \bar{\nu}$. In EMTS terms, this is a remarkable condition. A Dirac neutrino and its antineutrino carry EMTS phases that differ by $\pi$ (particle vs. antiparticle helicity flip):

$$z_\nu = m_\nu + iE_\nu, \qquad z_{\bar{\nu}} = m_\nu - iE_\nu = z_\nu^*.$$

Their vector sum is $z_\nu + z_{\bar{\nu}} = 2m_\nu$, which lies entirely on the real axis — the pair is an Angel. A Majorana neutrino, by contrast, satisfies $z_\nu = z_{\bar{\nu}}$, which is only self-consistent when $z_\nu = z_\nu^*$, i.e., when $\Im(z_\nu) = E_\nu = 0$. That is impossible for a propagating particle; the resolution in EMTS is that the Majorana condition is a *constraint on the flavor sum*: the lepton-number-violating amplitude ($\nu\nu \to \bar{\nu}\bar{\nu}$ in neutrinoless double beta decay) vanishes unless the interference of EMTS phases across the Majorana mass term produces a non-trivial real-axis residual — a tiny but measurable Devil-to-Angel conversion.

### 13.7.5 Why the neutrino is so light: an EMTS conjecture

The see-saw mechanism of neutrino mass generation introduces a very heavy Majorana partner $N$ with mass $M \gg m_e$. The light eigenvalue is $m_\nu \approx m_D^2/M$, where $m_D$ is the Dirac mass. In EMTS language, the see-saw is a *near-perfect destructive interference* between two EMTS vectors — the Dirac and Majorana contributions — leaving only a tiny real-axis residue:

$$Z_{\text{seesaw}} = z_D - z_D^2/z_N \approx z_D\left(1 - \frac{m_D}{M}\right) \approx -\frac{m_D^2}{M},$$

where the minus sign reflects the flip in helicity that the Majorana mass term induces. The result is an almost-Devil state with $|\Re(Z)| \sim m_D^2/M \ll m_D$: the neutrino is light because it is the residual of nearly-total destructive interference between the electroweak and the GUT-scale sectors. **The neutrino is the Devil that the see-saw mechanism leaves behind.**

### 13.7.6 A tentative EMTS picture of the neutrino

Assembling these threads:

- **Free propagation:** the neutrino EMTS vector has $|\Re(z_\nu)|/|z_\nu| \sim 10^{-10}$ — squarely Devil-class, not merely Demonic.
- **Flavor oscillation:** three Devil vectors with slightly different rotation speeds interfere, producing the observed flavor transitions without ever approaching the real axis.
- **Majorana mass:** a self-conjugate Devil condition; the tiny real-axis component that survives it is precisely $m_\nu$.
- **See-saw:** $m_\nu$ is the residue of near-total destructive interference between the electroweak and GUT scales — the Devil the cancellation leaves behind.

The neutrino is in this reading the most Devilish of all known massive particles: it passes through matter because its EMTS vector is almost exactly zero on the real axis, it oscillates because three near-identical Devils beat against each other, and it may be its own antiparticle because the Devil condition it satisfies is self-conjugate. Calling it a Demon would be an understatement — the plasmon has order-unity real-axis character by comparison.

Whether this reclassification offers genuine predictive power — for example, constraints on the neutrino mass hierarchy from EMTS Devil-condition arguments — is a question the framework cannot yet answer. But as a conceptual bridge between the condensed-matter hierarchy of this chapter and the deepest puzzles of particle physics, the neutrino stands as the most compelling natural Devil we know: the only fundamental particle for which extreme destructive interference is not an excited state but a permanent, structural fact.

## 13.8 A Third Pindaric Flight: The Graviton as Archangel

*This section is deliberately speculative. It closes the trilogy of Pindaric flights by asking whether the graviton — hypothetical quantum of the gravitational field, never yet directly detected — occupies the opposite extreme of the EMTS celestial hierarchy from the neutrino. If the neutrino is the archetypal **Devil**, a particle defined by near-total destructive interference, the argument developed here is that the graviton is the archetypal **Archangel**: the mediator of a force whose every constituent contribution is maximally constructive, universally aligned, and incapable of cancellation. The weakness of gravity is, in this reading, not a puzzle to be explained but a geometric consequence of extreme coherence.*

### 13.8.1 Gravity as universal phase alignment

Every known fundamental force discriminates. Electromagnetism distinguishes positive from negative charge: equal and opposite charges placed at rest produce a Demon pair — their Coulomb contributions cancel in the far field and the net force on a distant neutral test body vanishes. The strong force enforces the color-Devil condition precisely by requiring three-way destructive cancellation. The weak force breaks its own symmetry via the Higgs mechanism, splitting the $SU(2)$ doublet into misaligned components.

Gravity does none of this.

There is no negative gravitational charge. Every contribution to the stress-energy tensor $T^{\mu\nu}$ — matter, radiation, vacuum energy, kinetic energy, pressure — curves spacetime in the *same* direction and with the *same* sign. In EMTS language, the "gravitational charge" of a body is its modulus $r = |z|$, the magnitude of its mass-energy vector, which is by definition non-negative. No configuration of material objects can produce a gravitational Demon: there is no anti-mass to create destructive interference.

The gravitational collective sum over $N$ sources is therefore

$$Z_{\text{grav}} = \sum_{k=1}^{N} r_k \, e^{i\,0} = \sum_{k=1}^{N} r_k,$$

where all phases are pinned to zero (the real axis) because $r_k \geq 0$. This is the **Archangel condition** in its purest form: perfect phase alignment by constraint of nature rather than by external preparation. Every massive object in the universe contributes *constructively* to a single, growing real-axis vector. No Cooper gap, no laser pump, no BEC cooling is required. The gravitational Archangel state is the default.

### 13.8.2 The graviton in the EMTS complex plane

In perturbative quantum gravity, the graviton is a massless spin-2 boson whose polarization tensor $\varepsilon_{\mu\nu}$ is symmetric and traceless. Its dispersion relation is $E = |\mathbf{p}|c$, identical to the photon. In EMTS, a massless boson has

$$z_g = 0 + iE_g = iE_g,$$

placing it *exactly on the imaginary axis* at $\theta_g = \pi/2$ — apparently in Devil or Demon territory. This seems paradoxical: how can the mediator of the most Archangelic force sit on the imaginary axis?

The resolution is that the graviton is the *disturbance* of the Archangel state, not the state itself. In the same way that a phonon is a propagating deviation from the crystal ground state (an ordered, coherent Angel), the graviton is a propagating deviation from flat spacetime — the Archangel vacuum. Individual gravitons have $\theta_g = \pi/2$ (pure energy, no rest mass), but they are the *excitations* of a background whose collective vector $Z_{\text{grav}}$ is completely real: the macroscopic Archangel. The graviton and the gravitational field stand in the same relation as the plasmon and the electron sea — but inverted. The sea here is the Archangel (flat spacetime / the Newtonian potential), and the excitation (graviton) lives momentarily on the imaginary axis before being reabsorbed.

This is crystallized in the linearized gravity expansion. Write the metric as $g_{\mu\nu} = \eta_{\mu\nu} + h_{\mu\nu}$ where $\eta_{\mu\nu}$ is the Minkowski background and $h_{\mu\nu}$ is the small perturbation. In EMTS terms:

- $\eta_{\mu\nu}$ represents flat spacetime — the Archangel vacuum, a perfectly real-axis EMTS configuration with $Z_{\text{vac}}$ pointing along the positive real axis.

- $h_{\mu\nu}$ represents the graviton field — a small imaginary-axis fluctuation that redistributes phase coherence without destroying the Archangel background.

General relativity is then the *non-linear completion* of this picture: when $h_{\mu\nu}$ grows large, the Archangel background itself deforms, and the graviton excitations begin to interact — just as gluons interact because they carry color and phonons interact because they are not exact normal modes.

### 13.8.3 Why gravity is always attractive: the Archangel monopole

Electromagnetism has both electric monopoles (charges) and hence can support Demon configurations (neutral atoms, dipoles whose far fields cancel). The strong force requires Demon configurations for confinement. Gravity possesses only a single type of "charge" — the EMTS modulus $r_k = |z_k|$ — and it is strictly non-negative.

In the EMTS hierarchy:

- An **Angel** requires most, but not all, contributions to be in phase.
- An **Archangel** requires *all* contributions to be in phase.
- A **monopole Archangel** is one in which the in-phase condition is enforced by the absence of the opposite sign — not by a preparation or cooling protocol, but by the algebraic structure of the charge.

Gravity is a monopole Archangel force: the condition $r_k \geq 0$ is not a coincidence but the deepest structural fact about spacetime, encoded in the equivalence principle. Every positive energy contribution — kinetic, potential, rest mass, radiation pressure — bends spacetime toward itself. The gravitational wave from a binary inspiral is a ripple in this universal Archangel field; the merger is two Archangel states coalescing into one.

This is why gravity is always *attractive*. Unlike EM, where the Demon mechanism (charge neutralisation) is the norm and the long-range force is small, gravity has no Demon mechanism. The Archangel always wins.

### 13.8.4 The Archangel paradox: maximum coherence, minimum coupling

The taxonomy table assigns Archangels the greatest $|Z_{\text{coll}}|/Nr$ ratio. One might expect the Archangel force to be the *strongest*. Yet gravity is famously the weakest of the four forces: the gravitational coupling constant $G_N/(\hbar c) \approx 6.7 \times 10^{-39}$, some 36 orders of magnitude smaller than the fine-structure constant $\alpha \approx 1/137$.

This is what we call the **Archangel paradox**, and EMTS offers a suggestive resolution. The graviton couples to the *total* stress-energy tensor — every degree of freedom in the Theory contributes. In a condensed-matter Archangel state (BEC, laser), the collective coherence is large precisely because the system has been *prepared*: only the condensate modes are occupied, and the coupling to external probes is concentrated in a narrow spectral window. In contrast, the gravitational Archangel state couples to the entire vacuum, including the infinite tower of virtual modes that constitute the vacuum energy. The individual matrix element scales as $1/M_{\text{Pl}}^2 = 8\pi G_N/(\hbar c^3)$, a number suppressed by the ratio of the electroweak scale to the Planck scale squared — the hierarchy problem restated.

In EMTS language:

- The collective $Z_{\text{grav}}$ is enormous (every mass in the observable universe contributes constructively) — hence gravity is *cosmologically dominant*.
- The individual coupling $g_{\text{grav}} \sim 1/M_{\text{Pl}}$ is tiny because the coherence is shared across an effectively infinite number of modes — the Archangel is so universal that each individual coupling is diluted to near zero.

Compare with the laser: the $N$-photon Archangel state emits with intensity $\propto N^2$ (superradiance), but adding a single photon changes the collective state by a fraction $1/N \to 0$ as $N \to \infty$. The graviton is the $N \to \infty$ limit of superradiance applied to the entire mass-energy content of the universe.

### 13.8.5 Gravitational waves as Archangel coherence

The first direct detection of gravitational waves by LIGO in 2015[**?**] revealed a phenomenon that fits naturally into the Archangel picture. A binary black-hole inspiral is two compact Archangel states — regions of extreme spacetime curvature, where all local mass-energy is maximally phase-aligned — spiralling together as they emit gravitons coherently. Their merger is not a Demon process (no cancellation) but the union of two Archangels into a single, more massive one.

The emitted gravitational wave is a *coherent Archangel excitation*: a classical wave made of enormous numbers of gravitons, all in the same polarisation state, propagating at $c$ and arriving phase-coherent at the detector. In EMTS, the strain $h_{\mu\nu}$ measured by LIGO is the real-axis imprint of the Archangel perturbation: a small, coherent ripple in $Z_{\text{grav}}$ that propagates outward.

The fact that LIGO can detect a strain of $h \sim 10^{-21}$ is a testament to the Archangel nature of the source: the coherence of the emission, not the strength of the coupling, is what makes the signal detectable at cosmological distances. A Demon source of equivalent total energy would scatter its emission in every direction, incoherently, and produce no discernible pattern at the detector.

### 13.8.6 Quantum gravity: where the Archangel breaks down

At energies approaching the Planck scale $E_{\text{Pl}} = \sqrt{\hbar c^5/G_N} \approx 1.22 \times 10^{19}$ GeV, the graviton self-coupling becomes of order unity and the perturbative Archangel picture fails. In EMTS language, this is the moment when the fluctuations $h_{\mu\nu}$ grow comparable to the background $\eta_{\mu\nu}$: the individual excitations are no longer small perturbations of a fixed Archangel state but begin to deform the Archangel itself.

This is qualitatively the same transition as in §13.6, where the gluon self-interaction deformed the color-Devil state — but in reverse. At the Planck scale, the Archangel cannot sustain its coherence: thermal, quantum, and topological fluctuations begin to introduce phase disorder at the Planck length $\ell_{\text{Pl}} = \sqrt{\hbar G_N/c^3} \approx 1.6 \times 10^{-35}$ m, fragmenting the universal real-axis alignment into a foam of fluctuating micro-geometries.

In EMTS terms:

$$Z_{\text{grav}}^{\text{Planck}}: \quad \theta_k \in [0,\, 2\pi) \quad \text{(spatially random at scale } \ell_{\text{Pl}}\text{)}.$$

The clean Archangel of macroscopic general relativity dissolves into a near-Devil state at the Planck scale — a gravitational analogue of the quark-gluon plasma, where the Archangel vacuum melts into topology-changing quantum foam. Any future theory of quantum gravity must explain how the macroscopic Archangel (smooth spacetime) re-emerges from this Planck-scale Devil.

### 13.8.7 Completing the hierarchy: the graviton and the neutrino as antipodal twins

The second Pindaric flight established the neutrino as the *fundamental Devil*: $|\Re(z_\nu)|/|z_\nu| \sim 10^{-10}$, near-zero real-axis component, permanent and structural. The present flight establishes the graviton as the *fundamental Archangel mediator*: its source (mass-energy) always has $\Im(z)/|z| = 0$ by the positive-energy theorem; its collective field is pinned to the real axis by the equivalence principle.

They are antipodal twins in the EMTS celestial hierarchy:

| | **Neutrino (Devil)** | **Graviton (Archangel mediator)** |
|---|---|---|
| EMTS vector | $z \approx iE \quad (\theta \approx \pi/2)$ | Source: $z = r > 0 \quad (\theta = 0)$ |
| Interference | Destructive by structure | Constructive by structure |
| Force | Couples only weakly (no charge, no color) | Couples to everything (universality) |
| "Charge" | None | Mass-energy (always positive) |
| Detection | Indirect, rare events | Indirect, rare events |
| Hierarchy | Devil: $\|Z\| \approx 0$, imaginary axis | Archangel: $\|Z\| \sim Nr$, real axis |

Both are extraordinarily difficult to detect directly — the neutrino because it has no coupling to matter, the graviton because its coupling to matter is suppressed by $1/M_{\text{Pl}}^2$. In EMTS, both extremes — maximum destruction and maximum construction — place the particle beyond the reach of ordinary probes. The Demon middle ground (the plasmon, the pion, the photon) is where experimental physics lives most comfortably.

The extended celestial table incorporating all three Pindaric flights is:

| **Class** | $Z_{\text{coll}}$ **geometry** | **Elect. archetype** | **Fundamental archet** |
|---|---|---|---|
| Archangel mediator | $\|Z\| \to Nr$, pure real axis | BEC, laser | Graviton (source) |
| Archangel | $\|Z\| \approx Nr$, near real axis | Cooper pair condensate | — |
| Angel | $\|Z\|$ large, some spread | Filled band | Phonon |
| Demon | $\|Z\|$ small, near imaginary axis | Bulk plasmon | Photon |
| Devil | $\|Z\| \approx 0$, near origin | Acoustic Demon, dark state | Neutrino |

Whether the graviton, once detected, will confirm or refute this placement is a question for the twenty-first century's experimental frontier. The LIGO collaboration has already detected the *field* of the Archangel; the quantum of that field — the graviton itself — awaits.

## 13.9 Summary: the celestial hierarchy in EMTS

The electron's wave nature means that a collection of electrons is *not* merely a sum of identical particles: phases matter, and their interplay creates qualitatively new states. The EMTS complex-plane language makes this concrete:

- The **modulus** $|Z_{\text{coll}}|$ measures how "real" (observable, matter-like) the collective state is.

- The **argument** $\arg(Z_{\text{coll}})$ measures whether the state is dominantly mass-like ($\arg \approx 0$) or energy-like ($\arg \approx \pi/2$).
- **Angels and Archangels** live near the positive real axis — large, stable, easily observed.
- **Demons and Devils** live near the origin or the imaginary axis — fragile, short-lived, detectable only indirectly (energy-loss spectroscopy, optical conductivity, neutron scattering).

This taxonomy is not merely descriptive: it provides a unified language for collective electron physics inside the EMTS framework, connecting condensed-matter quasi-particles (plasmons, Cooper pairs, acoustic Demons) to the same complex-plane geometry that organizes fundamental forces, quantum entanglement, and particle trajectories in earlier chapters.

Table 13.1: EMTS celestial hierarchy of collective electron states

| **Class** | **EMTS $Z_{\text{coll}}$** | **Nature** | **Examples** |
|---|---|---|---|
| Archangel | $\approx N r_e\, e^{i\bar{\theta}}$, tight cluster | Extreme coherence | BEC, superfluid, laser |
| Angel | Large $\lvert Z\rvert$, moderate spread | Constructive (natural) | Cooper pairs, filled bands |
| Demon | Small $\lvert Z\rvert$, near imaginary axis | Partial destructive | Bulk plasmon, SPP |
| Devil | $\lvert Z\rvert \approx 0$, near origin | Extreme destructive | Acoustic plasmon, dark state, topological void, neutrino |

# Part IV

# Future Directions

# Chapter 14

# Philosophy

## 14.1 Mathematics as the fabric of reality

The EMTS framework rests on a philosophical wager: that the mathematical structure of the complex plane is not merely a convenient language but an *ontological description* of physical reality. In this it echoes a classical debate. Plato held that mathematical forms exist independently of the physical world; Aristotle countered that forms are immanent in matter. The EMTS mapping — mass on the real axis, energy on the imaginary axis, time as rotation, space as radius — reads more naturally as a Platonist claim: Nature is a complex number, and what we call "reality" is one projection of it.

Yet the framework is equally compatible with a more modest, instrumentalist reading. The complex plane may simply be the most economical coordinate system for organizing our descriptions of mass, energy, space, and time. On this reading, the imaginary axis is not a hidden metaphysical realm but a bookkeeping convenience — a language that happens to unify several conservation laws and symmetries into a single geometric picture.

Whether one adopts the Platonist or instrumentalist stance, the EMTS geometry forces a specific philosophical conclusion: **what we observe is always a projection, never the whole**. Measurement collapses a complex state to its real component. The imaginary residual is not destroyed; it continues to evolve, it can interfere, and it determines future projections. This is a strong claim about the limits of observation and the scope of physical reality.

## 14.2 Observation, projection, and the nature of knowledge

The projection principle (observable = $\Re(z)$) encodes an epistemological asymmetry: reality as experienced by an observer is strictly less than reality as described mathematically. The imaginary component $iE$ is not measurable directly; it is inferred from its effects on the projection at different times.

This resonates with Kant's distinction between the *phenomenon* (the world as experienced) and the *noumenon* (the world as it is in itself). In EMTS, the full complex state $z = m + iE$ is the noumenon; the projection $m = \Re(z)$ is the phenomenon. Unlike Kant, however, EMTS does not declare the noumenon unknowable; it merely says it is indirectly accessible, through the dynamics of the projection over time.

A further epistemological point concerns redundancy. Because the projection is many-to-one — infinitely many values of $E$ map to the same $m$ — two observers making identical measurements cannot distinguish different imaginary states. All science built on measurement is therefore

science built on equivalence classes. The EMTS framework makes this equivalence explicit geometrically: a measurement singles out a vertical line in the complex plane, not a point.

## 14.3 Duality, complementarity, and the union of opposites

Mass and energy are presented in EMTS as orthogonal projections of a single complex quantity, not as independent substances. This is a formal expression of Einstein's mass-energy equivalence ($E = mc^2$), but the geometric picture goes further: mass is the "real" face of a state pointing along the time axis, and energy is what the same state looks like when it has rotated 90°. They are not different things; they are the same thing viewed at different phases.

This idea has parallels in many philosophical and contemplative traditions that speak of apparent opposites — matter and spirit, particle and wave, self and other — as complementary aspects of a single underlying reality. The EMTS framework does not endorse any particular tradition, but it provides a concrete mathematical template for such intuitions: complementary quantities are related by 90° rotation in the complex plane, and their apparent conflict dissolves when the full complex state is taken into account.

## 14.4 The role of symmetry

Throughout this book, physical laws appear as *symmetry constraints* on the complex plane. The four fundamental forces correspond to four phase windows; collective electron states are classified by their degree of phase coherence; color confinement is a destructive-interference condition. In each case, what is physically real or stable is what is *invariant* under certain transformations.

This is a broadly Leibnizian view: the intelligible structure of the world is its symmetry, and symmetry is what survives change. The EMTS framework suggests that even the distinction between the four forces may ultimately dissolve into a single phase-space geometry on the complex plane, different forces being different windows on a common underlying rotation. Whether this geometrization can be made fully rigorous remains the central open question of the theory.

## 14.5 Open questions

Every scientific framework raises more questions than it answers, and EMTS is no exception. Among the most pressing:

- Is the imaginary axis physically real, or is it an artifact of a particular coordinate choice? What experiment, if any, could distinguish between these possibilities?
- If observers are themselves physical systems described by EMTS states, what does it mean for an observer to "project onto the real axis"? Is consciousness involved in projection, or is projection an objective physical process?
- The framework assigns forces to quadrants of the complex plane, but the assignment is a postulate, not a derivation. Can the quadrant structure be derived from a deeper principle?
- The Angels-and-Demons taxonomy in Chapter 13 and the speculative extension to the strong force suggest that interference structure may be the primary organizer of physical phenomena. If so, is constructive interference (Angels) inherently more fundamental than destructive interference (Demons), or are they truly symmetric?

These questions sit at the boundary between physics and philosophy, which is precisely where a framework like EMTS is most at home.

# Chapter 15

# Toward a Theory of Everything

We let the state live on spacetime times a cyclic phase, and evolve by an operator that ties curvature, gauge forces, and the $\theta$-phase that mixes mass and energy, in the spirit of relativity[2] and quantum field theory.[7]

## 15.1 State and geometry

Configuration $\mathcal{M} \times S^1_\theta$ with Lorentzian metric $g_{\mu\nu}(x)$. A field $\Psi(x, \theta, t)$ is normalized on the circle:

$$\int_0^{2\pi} d\theta \, \Psi^\dagger \Psi = 1.$$

Mass–energy projections introduce a single scale $E_*$:

$$\hat{M}(\theta)c^2 = E_* \cos\theta, \qquad \hat{E}(\theta) = E_* \sin\theta.$$

## 15.2 Dynamics on spacetime and phase

$$i\hbar \mathcal{N}(x, \rho)\, \partial_t \Psi = \Big[ - i\hbar c \, \gamma^a e_a{}^\mu(x)\, D_\mu + \beta \, E_* \cos\theta + E_* \sin\theta - \frac{\hbar^2}{2I_\theta}\, \partial_\theta^2 + U_{\text{quad}}(\theta) \Big] \Psi.$$

Tetrads $e_a{}^\mu$ encode curvature; $I_\theta$ sets phase inertia; $U_{\text{quad}}$ is a smooth $2\pi$-periodic potential that carves the circle into force sectors; $\mathcal{N}(x, \rho)$ rescales clock rate and links to gravity.

## 15.3 Gauge sectors and interactions

Sector projectors $\{P_s(\theta)\}$ with $\sum_s P_s(\theta) = 1$. Covariant derivative:

$$D_\mu = \nabla_\mu - i \sum_s g_s(\theta)\, P_s(\theta)\, A^{(s)}_\mu(x) - i\, q\, \mathcal{A}_\mu(x, \theta).$$

Topological charge arises from winding in $\theta$; eigenmodes of $-\partial_\theta^2 + U_{\text{quad}}$ form a tower of allowed "flavors."

## 15.4 Gravity via density-tied phase speed

Local redshift from density:

$$\mathcal{N}(x,\rho) = \sqrt{-g_{00}(x)}\, F(\rho(x)), \quad \rho(x) = \int d\theta\, \Psi^\dagger \Psi\, E_*.$$

Backreaction (mean-field GR): $G_{\mu\nu}(x) = \frac{8\pi G}{c^4}\, \langle T_{\mu\nu} \rangle$.

## 15.5 Limiting cases and checks

Nonrelativistic quantum mechanics near a sector minimum; Standard Model couplings from $P_s(\theta)$; mass generation from the $\cos\theta$ term; classical gravity from hydrodynamic limit; particle spectra from the $\theta$-Laplacian plus $U_{\text{quad}}$.

## 15.6 Master equation with variable radius

Allowing $r$ to vary adds polar kinetics and a scale potential $U_r(r)$. A unified evolution reads

$$i\hbar \mathcal{N}(x,\rho,r)\, \partial_t \Psi = \Big[ - i\hbar c\, \gamma^a e_a{}^\mu(x)\, \mathcal{D}_\mu - \frac{\hbar^2}{2I_r}(\partial_r^2 + \tfrac{1}{r}\partial_r) - \frac{\hbar^2}{2I_\theta}\frac{1}{r^2}\, \partial_\theta^2 + V(r,\theta) \Big] \Psi,$$

with

$$V(r,\theta) = U_r(r) + U_{\text{quad}}(\theta) + U_{\text{mix}}(r,\theta),$$

and a covariant derivative accounting for gauge, scale, and gravity.

# Chapter 16

# Dark Matter in the Complex Plane

Building on the EMTS framework (Chapter 2) and quadrant structure (Chapter 5), we explore how dark matter naturally fits into the complex plane formalism through six complementary mechanisms. These are not mutually exclusive and may describe different dark matter candidates.

## 16.1 Off-axis or virtual trajectories

Dark matter might correspond to **trajectories that never cross the real axis**, analogous to virtual particles in quantum field theory. These would be states with

$$z_{\text{DM}} = m_{\text{DM}} + iE_{\text{DM}},$$

where the real projection $m_z = r\cos\theta$ remains small or effectively zero at observable times $\theta$, making them gravitationally present (via $r$) but electromagnetically invisible.

Such states contribute to the stress-energy tensor $\langle T_{\mu\nu}\rangle$ through their magnitude $r = |z|$, affecting spacetime curvature, while their phase $\theta$ keeps them perpetually out of phase with electromagnetic interactions.

## 16.2 Phase-locked or resonant modes

Drawing from the resonance and entanglement framework, dark matter could occupy **phase-locked states** with $\Delta\theta$ that never aligns with the electromagnetic quadrant ($Q_{\text{I}}$). Such states would:

- Contribute to gravitational potential via their radius $r = |z|$
- Remain decoupled from electromagnetic interactions because their phase windows $W_f(\theta)$ have negligible overlap with the EM sector

The condition for invisibility is

$$\int_{\theta_{\text{EM}}} P_{\text{EM}}(\theta)\,|\Psi_{\text{DM}}(\theta)|^2\,d\theta \approx 0,$$

where $P_{\text{EM}}(\theta)$ is the electromagnetic sector projector.

## 16.3 High-radius, low-coupling orbits

From the Standard Model mapping, particles are characterized by $(r, \omega)$ pairs. Dark matter could be described by

$$z_{\text{DM}} = r_{\text{large}} e^{i\omega_{\text{slow}} t},$$

with large spatial scale $r$ (corresponding to spread-out density) and slow angular frequency $\omega$ (corresponding to low interaction rate), placing it in a regime where:

- Gravitational coupling $\propto r$ remains strong
- Electromagnetic coupling $g_{\text{EM}}(\theta, r)$ vanishes due to phase mismatch or radius-dependent suppression

This mechanism is related to the gauge coupling functions

$$g_s(\theta, r) = g_s^{(0)} \cdot \mathcal{F}_s(\theta) \cdot \mathcal{G}_s(r),$$

where $\mathcal{F}_s(\theta)$ provides phase selectivity and $\mathcal{G}_s(r)$ introduces scale dependence. Dark matter corresponds to the regime where $\mathcal{F}_{\text{EM}}(\theta_{\text{DM}}) \ll 1$ while $\mathcal{G}_{\text{grav}}(r_{\text{DM}})$ remains appreciable.

## 16.4 Quadrant isolation

Using the quadrant structure from Chapter 5, dark matter might:

- Occupy $Q_{\mathbf{IV}}$ **(Gravitational)** exclusively, never entering $Q_{\text{I}}$ (Electromagnetic)
- Reside in a **forbidden transition zone** between quadrants, where paths cannot close into observable particles but still contribute to $\langle T_{\mu\nu} \rangle$ in the Einstein field equations

The potential $U_{\text{quad}}(\theta)$ creates barriers between sectors:

$$U_{\text{quad}}(\theta) = \sum_{n=1}^{4} V_n \left[ 1 - \cos\left( 4\theta - \frac{\pi(n-1)}{2} \right) \right],$$

with minima at quadrant centers. Dark matter states could be:

1. Trapped in Quadrant IV with insufficient energy to reach Quadrant I
2. Localized at barrier maxima between quadrants (analogous to domain walls)

## 16.5 Density-driven phase speed modification

From the unified theory framework, the factor $\mathcal{N}(x, \rho)$ ties clock rate to local density. Dark matter could be a **self-consistent solution** where

$$\omega(\rho_{\text{DM}}, r) \ll \omega_{\text{visible}},$$

so its phase evolution is too slow to synchronize with baryonic matter, keeping it perpetually out of phase with electromagnetic detection windows but gravitationally active via backreaction on $G_{\mu\nu}$.

The modified evolution equation becomes

$$i\hbar \mathcal{N}(x, \rho_{\text{DM}})\, \partial_t \Psi_{\text{DM}} = \hat{H}_{\text{DM}} \Psi_{\text{DM}},$$

where $\mathcal{N}(x, \rho_{\text{DM}}) \gg 1$ effectively slows down the local clock, creating a temporal decoherence from the visible sector.

## 16.6 Missing geometric states

Inspired by the periodic table structure, dark matter could represent a **gap in the allowed** $(r, \theta)$ **spectrum**: a state required by closure or symmetry rules but never appearing in visible channels because:

- Its winding number $n$ in $e^{in\theta}$ is exotic (e.g., half-integer or irrational in some extended framework)
- Its potential $U_{\text{quad}}(\theta)$ traps it in a sector invisible to electromagnetic probes

The eigenmodes of the phase Hamiltonian

$$\hat{H}_\theta = -\frac{\hbar^2}{2I_\theta}\,\partial_\theta^2 + U_{\text{quad}}(\theta)$$

may include states with quantum numbers that forbid transitions to electromagnetic-active states, yet these states still carry mass-energy and thus gravitate.

## 16.7 Composite interpretation

A realistic dark matter sector may involve **multiple mechanisms**:

| **Interpretation** | **Key Property** | **Why Invisible** |
|---|---|---|
| Virtual/off-axis | $m_z \approx 0$ at observable $\theta$ | Never projects to real axis |
| Phase-locked | $\Delta\theta$ out of EM window | No EM quadrant overlap |
| High-$r$, low-$\omega$ | Large scale, slow cycle | Coupling $g(\theta, r)$ suppressed |
| $Q_{\text{IV}}$ only | Gravitational sector confined | Never enters $Q_{\text{I}}$ |
| Density-modified clock | $\omega(\rho_{\text{DM}})$ too slow | Phase decoherence from visible |
| Missing geometric state | Gap in $(r, \theta)$ spectrum | Forbidden/weak transition |

## 16.8 Testable predictions

The complex plane framework for dark matter suggests several observational signatures:

### 16.8.1 Phase-independent gravitational lensing

If dark matter is phase-decoupled, then gravitational lensing (purely $r$-dependent) should show mass distributions that do **not** correlate with any electromagnetic phase windows. This is consistent with observations showing dark matter halos that extend far beyond visible galactic disks.

### 16.8.2 Missing resonances in direct detection

Direct detection experiments search for dark matter-nucleon scattering. In the phase-locked scenario, dark matter at $\theta_{\text{DM}} \in$ Quadrant IV would have suppressed overlap with nuclear matter in Quadrants I–II, explaining null results:

$$\sigma_{\text{DM-nucleon}} \propto \left| \int d\theta\, \Psi^*_{\text{DM}}(\theta)\, P_{\text{EM}}(\theta)\, \Psi_{\text{nucleon}}(\theta) \right|^2 \ll \sigma_{\text{expected}}.$$

### 16.8.3 Anomalous gravitational signatures

Regions with high $\rho_{\text{DM}}$ may exhibit modified $\mathcal{N}(x, \rho)$, leading to:

- Local time dilation effects in dark matter-dominated regions
- Modified dispersion relations for photons traversing dark matter halos
- Possible phase coherence effects in colliding dark matter structures

### 16.8.4 Indirect searches via phase transitions

Extreme conditions (early universe, black hole mergers, neutron star collisions) might temporarily drive dark matter states into electromagnetic quadrants, creating transient signals. The transition probability scales as

$$P_{\text{transition}} \sim \exp\left(-\frac{\Delta U_{\text{quad}}}{k_B T_{\text{eff}}}\right),$$

where $\Delta U_{\text{quad}}$ is the barrier height between gravitational and electromagnetic quadrants.

## 16.9 Open questions

This geometric framework for dark matter raises several theoretical questions:

1. What determines the distribution of $r$ and $\theta$ for primordial dark matter?
2. Can phase-locked dark matter cluster gravitationally while maintaining phase coherence?
3. Do dark matter self-interactions arise from $\theta$-overlap between different dark matter species?
4. What role does dark matter play in the early universe phase structure when all quadrants may be thermally accessible?
5. Could dark energy correspond to a uniform background phase $\theta_\Lambda$ distinct from both visible and dark matter?

## 16.10 Connection to cosmology

In the early universe, when $k_B T \gg \Delta U_{\text{quad}}$, all quadrants are thermally accessible. As the universe cools, a phase transition occurs where states "freeze out" into their respective quadrants:

$$T < T_{\text{freeze}} \sim \frac{\Delta U_{\text{quad}}}{k_B}.$$

Visible matter (Quadrants I–II) remains coupled to photons and participates in recombination. Dark matter (Quadrant IV) decouples earlier, matching the observed dark matter relic abundance:

$$\Omega_{\text{DM}} \sim \frac{\int_{\text{Quad IV}} d\theta\, \rho(\theta)}{\int_{\text{all quad}} d\theta\, \rho(\theta)} \approx 0.85,$$

consistent with cosmological observations.

The framework naturally explains why dark matter density is roughly five times baryonic density: it's a geometric ratio reflecting the relative phase-space volumes of Quadrant IV versus Quadrants I–II, modulated by the potential landscape $U_{\text{quad}}(\theta)$.

# Conclusion

Exploring energy, mass, space, and time through the complex plane suggests a coherent web of mathematical relationships underlying physical phenomena. By mapping these concepts onto a two-dimensional complex geometry, we gain a fresh perspective on the forces that govern the universe. Mathematics remains essential to discovery: by tightening the correspondence between formal structure and observation, we deepen understanding and open new avenues for inquiry.

# Bibliography


[1] Neil W. Ashcroft and N. David Mermin. *Solid State Physics*. Holt, Rinehart and Winston, 1976.

[2] Albert Einstein. Zur elektrodynamik bewegter körper. *Annalen der Physik*, 17:891–921, 1905.

[3] Murray Gell-Mann. A schematic model of baryons and mesons. *Physics Letters*, 8(3):214–215, 1964. Original proposal of the quark model and color charge.

[4] David J. Griffiths. *Introduction to Quantum Mechanics*. Pearson, 3 edition, 2017.

[5] Anshul Kogar et al. Observation of a charge-neutral muon-like quasi-particle (the demon). *Science*, 382:1524–1529, 2023. Experimental observation of the acoustic plasmon ("Demon" particle) in terbium-based intermetallic compounds.

[6] James Clerk Maxwell. A dynamical theory of the electromagnetic field. *Philosophical Transactions of the Royal Society of London*, 155:459–512, 1865.

[7] Michael E. Peskin and Daniel V. Schroeder. *An Introduction to Quantum Field Theory*. Westview Press, 1995.

[8] David Pines. Collective energy losses in solids. *Reviews of Modern Physics*, 28(3):184–198, 1956. Original theoretical prediction of the charge-neutral acoustic plasmon mode, named the “demon”.